Atmospheric forcing of the southeast Bering Sea Shelf during 1995–99 in the context of a 40-year historical record

N.A. Bond [1] and J.M. Adams[1,2]

[1] Joint Institute for the Study of the Atmosphere and Oceans
Box 354235
University of Washington
Seattle, WA 98195-4235

[2] Now at: Center for Ocean-Land-Atmosphere Studies
4041 Powder Mill Road, Suite 302, Calverton, MD 20705-3106

For submission to Deep-Sea Research II: Topical Studies in Oceanography

12 February 2001

Contribution #2257 from NOAA/Pacific Marine Environmental Laboratory

Abstract

The atmospheric forcing of the Bering Sea over its eastern shelf is estimated using the 40-year record of daily data from the NCEP/NCAR Reanalysis. This data set includes estimates of the processes responsible for the atmospheric forcing, namely the surface fluxes of momentum, sensible and latent heat, and longwave and shortwave radiation, and therefore permits quantifying effects that previously could only be inferred from the large-scale nature of the flow. The forcing in 1995 through 1999 is described in detail using daily time series; historical context for these results are provided with seasonal averages for the years 1959 through 1999.

The analysis for winter concentrates on aspects related to formation and advection of sea ice. Results indicate that the presence of sea ice is strongly related to the net surface heat fluxes as well as the cross-shelf component of the wind. The 40-year record lacks any discernible long-term trend in the winter forcing and response. There was a notably cold period in the early to middle 1970s, and a warm period from the late 1970s into the early 1980s, but conditions during the 1990s are similar to those in the late 1950s and 1960s.

The analysis for the warm season focuses on the mechanisms responsible for the variability in SST warming. Much of the intraseasonal and interannual variability in this warming can be attributed to variations in the downward shortwave radiation (solar heating). The 40-year record does indicate a long-term trend toward increased solar heating, and reduced surface latent heat fluxes (evaporative cooling). These changes have led to August SSTs in the 1990s that are roughly 1°C warmer than in the 1960s.

Keywords: Air-sea interaction, climatic changes, weather

1. Introduction

An impressive set of physical, chemical, and biological observations were collected on the Bering Sea shelf from 1995 through 1999. These observations have been used to examine the linkages between different elements of the shelf's marine ecosystem under a variety of conditions (as summarized in this volume by Hunt et al., 2001). The present paper has two objectives: to document in detail the atmospheric forcing of the Bering Sea shelf during the 1995–99 period of intensive observations, and to examine this period in the context of the historical climate record. Our results should aid interpretation of the findings by the other investigators, as reported in the companion papers in this volume. Our results also suggest a long-term trend in the warm-season climate of the eastern Bering Sea.

Most of the previous work on the variability in air-sea interactions of the Bering Sea has concerned the entire North Pacific basin during the winter season (e.g., Graham, 1994; Trenberth and Hurrell, 1994; Zhang et al., 1997, among many others). There have been a few studies on the variability in sea ice over the Bering Sea shelf (Niebauer et al., 1999, and references therein) and a study of the causes of the unusually warm summer of 1997 in the eastern Bering Sea (Overland et al., 2001a). But for the most part, existing information focuses on how the large-scale winter mean climate has evolved, with an emphasis on the "regime shift" in the middle to late 1970s. The marine ecosystem must be sensitive to the variability in atmospheric forcing in the spring and summer as well as in the winter, and hence warm season variability merits scrutiny.

A detailed analysis of recent air-sea interactions over the shelf is compelled not only by the other research reported in this volume, but also by the tools that have lately become available. The development of multi-decade data sets such as the National Center for Environmental Prediction (NCEP)/National Center for Atmospheric Research (NCAR) Reanalysis (Kalnay et al., 1996) has made it feasible to study aspects of the air-sea interaction directly. Reanalyses provide estimates of the physical processes involved in air-sea interaction, namely the mechanisms responsible for the exchange of heat, water, and momentum. These estimates are

calculated on a daily basis at local spatial scales (~200 km). Air-sea interaction studies no longer need to be restricted to gross aspects of the atmosphere-ocean system, as encapsulated by indices such as the Pacific-North American pattern (PNA) or Pacific Decadal Oscillation (PDO). There is still a definite value in considering these indices, since they represent the fundamental modes of the climate system. A companion paper (Overland et al., 2000b) considers how the various aspects of the atmospheric forcing detailed here relate to modes of climate variability.

The paper is organized as follows. Section 2 describes the NCEP/NCAR Reanalysis data set and the results of some local validation tests. Section 3 presents the daily atmospheric forcing for the period 1995–99. Winter and spring/summer are considered separately since different mixes of processes are important at different times of year. The historical context for these daily time series is provided in section 4, using seasonal averages for winter and spring/summer for the period 1959 through 1999. We conclude with a discussion (section 5) and a summary (section 6).

2. The NCEP/NCAR Reanalysis Data Set

Our analysis is based on a 40-year record of atmospheric variables from the NCEP/NCAR Reanalysis data set (Kalnay et al., 1996). This data set was produced using a state-of-the-art numerical weather prediction model and data assimilation system incorporating available surface, upper-air, and satellite-based observations. The consistency in the procedure used for the reanalysis makes it well-suited for studying climate variability from short-term to decadal timescales. There are two classes of output fields: (1) prognostic variables that are closely constrained by observations, e.g., wind and pressure, and (2) diagnostic variables, which are not directly observed but derived from the general circulation model used in the data assimilation, e.g., radiative heat fluxes. The diagnostic variables are prone to greater errors, but various studies (e.g., Yang et al., 1999; Adams et al., 2000) indicate that a large fraction of these errors are due to systematic biases. These types of biases tend to be removed in calculations of anomalies (only non-linear aspects of systematic errors will be retained), and hence have

minimal impacts on evaluations of variability.

The quality of the reanalysis data in the Bering Sea can be directly evaluated using measurements collected by a moored buoy on the Bering Sea shelf (Reed and Stabeno, 2001, this volume). These measurements were not assimilated in the reanalysis, and hence represent an independent data set for validation. The top panels of Fig. 1 display daily averages of the meridional component of the surface wind from Mooring 2 at 57°N, 164°W and from the reanalysis for April through September of 1996 and 1999. The variability on daily to weekly timescales is well-represented in the reanalysis; the correlation coefficient between these time series is 0.95 in 1996 and 0.94 and 1999. This is not surprising, since the pressure patterns producing these winds occur on scales of ~1000 km, and are reasonably well-sampled by the operational observing network. Fortunately, the observational record from Mooring 2 also allows evaluation of one of the most important diagnostic variables, the downward shortwave (solar) radiative heat flux. This component of the net surface heat flux dominates the heating of the water column in summer (Reed and Stabeno, 2001, this volume). Comparisons between the measurements at Mooring 2 and the estimates from the reanalysis for 1996 and 1999 (bottom panels of Fig. 1) reveal good but not excellent agreement. The reanalysis captures the weekly variability but sometimes misses the shorter-term variability. The correlation coefficient between the two time series is 0.70 in 1996 and 0.55 in 1999. These correlations are significant at the 99% confidence level (assuming an auto-correlation timescale of roughly 5 days or 30 degrees of freedom each year). The reanalysis does systematically overestimate the shortwave fluxes from mid-July through mid-September. Shallow sea fog is common over the Bering Sea during this time of year and the reanalysis may not be properly accounting for its presence and effects. It is also possible that the measured solar radiation is generally lower late in the mooring's deployment due to degradation (fouling) of the sensor (P. Stabeno, personal communication). Since these sources of error are more systematic than random, the temporal variability in the shortwave flux appears to be well represented in the reanalysis.

Time series of reanalysis data for the winter and spring/summer seasons are presented in

the following two sections. The parameters of greatest interest during the winter season (December–April) are related to the formation and advection of sea ice. The focus for the spring/summer season (May–September) is on parameters relevant to the rate of SST warming. The time series in section 3 are daily averages for 1995 through 1999, the years of enhanced observations in the Bering Sea. The time series in section 4 consist of seasonal averages for the 40-year period 1959–1999. The various parameters are evaluated mostly at the grid cell closest to the Mooring 2 site at 57°N, 164°W (Fig. 2); this location is representative of the entire Bering Sea shelf given the characteristically broad scales of atmospheric structure. One exception is the time series of heat fluxes in winter, which are evaluated in the eastern portion of the deep basin of the Bering Sea (56°N, 172°W). This location reflects the atmospheric conditions farther east over the shallow waters of the shelf, but does not experience sea ice. The presence of sea ice drastically reduces the surface fluxes of sensible and latent heat; the air and top of the ice reach equilibrium, but heat continues to be transferred from the ocean to the bottom of the ice. The surface fluxes over the deep basin where sea ice does not form are a proxy for the effective cooling of the upper ocean over the shelf when sea ice is present. Parameters related to the wind-forced ocean circulation of the southeast Bering Sea are also evaluated at locations other than Mooring 2; these locations are also indicated in Fig. 2.

3. Daily Forcing 1995–1999

This portion of the analysis documents the detailed evolution of the atmospheric forcing over the Bering Sea shelf, and the associated response in the SST. Daily time series are necessary to fully resolve the highly episodic nature of the forcing and response. The exact timing of particular events can be important to the physical oceanographic system (as discussed in this volume by Kachel et al., 2001 and Stabeno et al., 2001b). We presume that this timing can also be of importance to the marine ecosystem, and that the time series presented below are of relevance to some of the other studies in this volume.

a. Winter

The wintertime atmospheric forcing related to sea ice is crucial to the Bering Sea shelf. Sea ice influences the state of the entire physical system during winter, as well as important elements of the shelf's ecosystem into the following spring and summer (e.g., Wyllie-Echeverria and Wooster, 1998). Pease (1980) showed that sea ice over the shelf is controlled by two mechanisms: the off-shelf component of the surface wind stress, which determines the advection of sea ice out of its region of generation in coastal polynyas, and the net surface heat flux, which measures the rate of cooling of the ocean by the atmosphere. The net surface heat flux is the combination of the fluxes of sensible and latent heat and the net longwave and shortwave radiative fluxes. The reanalysis surface temperatures reflect the ice surface temperature when ice is present, and the SST otherwise, thus providing a measure of the extent and duration of the sea ice over the shelf. Daily time series of surface temperature, net surface heat flux, and cross-shelf wind stress for December through April for the years 1995 through 1999 are shown in Figs. 3a–e. Climatological means (1959–1999) for these quantities are also plotted for reference. The maximum ice extent during each of these winters is plotted in Fig. 2.

The time series for December 1994 through April 1995 (Fig. 3a) shows two periods of ice at Mooring 2, a 2-week event from late January into early February and a 3-week event in late March. Off-shelf wind anomalies and negative heat flux anomalies accompanied both events. There was some preconditioning (i.e., enhanced negative heat fluxes) for the latter event in the second week of March. In part due to this preconditioning, and because upper ocean heat contents tend to be at their minimum in March, relatively modest cooling and a short period of off-shelf wind anomalies were able to bring about a fairly long spell of ice to the location.

Persistently warm conditions prevailed in the winter of 1996 (Fig. 3b). Only a bit of sea ice occurred briefly in the second week of February. Although a period of strong off-shelf winds and large heat fluxes occurred in early January, it was not accompanied by any sea ice; this lack of ice might be attributable to the persistently weak heat fluxes during December. Anomalously weak heat fluxes and on-shelf winds from mid-February through March brought about surface

temperatures ~4°C warmer than normal and prevented much of a response to the period of strong off-shelf winds in early April.

The winter of 1997 (Fig. 3c) was typical of those in the recent past. There were three periods of sea ice of 4–12-day duration, each in association with significant off-shelf wind anomalies. The first two events also included greater heat fluxes for local cooling of the ocean; this mechanism may not have been necessary for the third ice event because the water column was already near freezing. As in many winters, a period of off-shelf winds and large heat fluxes in early January did not result in any ice at the Mooring 2 location. Extraordinary weather is required to bring sea ice to this location before late January.

The winter of 1998 (Fig. 3d) was relatively cold early, with sea ice mostly present from late January until early March, and then turned relatively warm from early March through April. The early and extensive ice may be attributable to the persistent off-shore winds from early December through January. The anomalous near-surface flow from the north results in cooler upper ocean temperatures. The rapid warming in March is associated with a shift to anomalously weak surface heat fluxes and later in April, a shift to on-shelf (southerly) winds.

The times series for the winter of 1998–99 (Fig. 3e) shows an abrupt onset of ice near the first of February, thawing in mid-February, and the return of ice from the start of March into early April. There are hints of the presence of ice as late as the end of April. This late sea ice hampered research ship activities over the shelf during April and May of 1999 (P. Stabeno, personal communication). The largest on-shelf wind event of the five winters occurred in the latter part of January. This produced an actual warming of the SST at a time of year when cooling predominates, presumably due to the advection of warmer water from the south.

b. Spring and Summer

The rate of upper ocean warming in the spring and summer over the Bering Sea shelf is important to the marine ecosystem. The warming of the upper mixed layer modifies the stratification, which in turn influences the exchange of water from below, and ultimately,

biochemical processes. Here we examine the SST warming rate, i.e., the temperature tendency, and two of its important and episodic forcing mechanisms. A 5-day running mean filter is applied to the SST tendency to smooth out its high-frequency variations, which are not resolved by the SST data used in the reanalysis (Reynolds and Smith, 1994). The two forcing mechanisms considered here are the wind mixing or u_*^3, where $u_* = (\tau/\rho)^{1/2}$ is the friction velocity, and the downward shortwave radiation flux at the surface. The former quantity is proportional to the rate of mechanical energy applied at the ocean surface for stirring; the latter quantity is the principal source of atmospheric heating for the ocean in the spring and summer. Daily time series are presented for May through September of 1995 to 1999 in Figs. 4a–e.

The spring and summer of 1995 (Fig. 4a) featured above normal SST tendencies during most of June and much of July. This anomalous warming can be attributed to very little wind mixing, and hence reduced entrainment of cooler water from below the thermocline. In addition, the downward shortwave flux or insolation tended to be greater than normal. Relatively typical conditions occurred in August and September.

The SST tendency during 1996 (Fig. 4b) was near its climatological mean in an overall sense, with substantial fluctuations from June through mid-July. This was a stormy summer on the whole, with seasonally strong wind mixing through much of the period and especially prominent wind events in the second half of June and in September. The insolation was near normal over periods longer than a few days, aside from a period in late June when it was ~50 W m^{-2} below normal. This coincided with an interval of negative anomalies in SST tendency.

The summer of 1997 is noteworthy for its large warm SST anomalies (Stabeno et al., 2001a), which has been linked to the strong El Niño of 1997–98 (Overland et al., 2001a). Figure 4c shows that most of the anomalous warming took place during three separate segments lasting 10 to 15 days, with an especially prominent positive anomaly occurring near the end of May. After a week of very strong winds in mid-May, there were generally low wind speeds until the end of August. Shortwave flux anomalies averaged ~50 W m^{-2} greater than normal from late May to mid-July. The consequence of enhanced solar heating and the lack of wind mixing was

record warm SSTs over the shelf by the middle of August.

Fairly typical SST tendencies occurred for 1998 as a whole (Fig. 4d). There were two periods of anomalous warming in June and July, followed by periods of negative anomalies from the end of July into early September. This cooling was associated with the significant wind mixing in August brought on by the early onset of the stormy season. The shortwave fluxes averaged a bit less than normal, with prominent negative anomalies from late May into June and during the storms of August and September.

The SST tendencies during spring and summer of 1999 (Fig. 4e) were, on the average, near the climatological mean. There were anomalously positive tendencies from mid-June through August, and two significant negative anomalies in late July and the first week of August. The latter anomaly occurred during the only significant wind mixing event of the season; for the most part, the spring/summer of 1999 was meteorologically quiet. The shortwave radiative fluxes exhibited the usual short-term (less than a week) fluctuations of 20–50 W m^{-2}.

4. Seasonal Averages 1959–1999

a. Winter

Figure 5 shows 40-year records of seasonal means of several variables that summarize the interannual variability of the surface conditions over the middle shelf. To aid in the interpretation of any climatological trends, the variables are plotted as departures from the 40-year mean. As mentioned earlier, the reanalysis surface temperatures provide an indicator of the extent and duration of sea ice over the shelf. The 40-year time series of mean winter (Jan–Apr) temperature anomalies (top panel of Fig. 5) shows a cold period from 1971 through 1976 followed by an extended warm period from 1977 through 1987. This change in the local climate is the signature of the North Pacific "regime shift" documented by Mantua et al. (1997), among others. Over the 40-year period, however, the time series includes virtually no trend. In the 1960s and 1990s, the seasonal mean surface temperatures at Mooring 2 were close to their climatological mean of -–3.6°C.

It is instructive to compare the surface temperature time series with seasonal averages for the cross-shelf wind stress and net heat flux (the parameters assumed to largely control sea ice and whose daily values were presented in the previous section). The winter mean anomalies (January through April) for the cross-shelf wind stress and net heat flux (middle panel of Fig. 5) exhibit significant interannual and some decadal variability. The anomalous cross-shelf wind stress (solid line) is only weakly correlated with the mean temperature (R ~0.3; which is significant at the 95% level). The wind stress was strongly negative (implying northeast winds) during the cold winters of the early 1970s, but comparable stresses in the late 1980s were accompanied by mostly climatological temperatures and sea ice concentrations. The anomalous net heat flux (dashed line) is better correlated with the mean temperature (R ~0.6; which is significant at the 99.9% level).[1]

The cold period from 1971 through 1976 coincided with enhanced heat fluxes, and the warmth of the late 1970s and 1980s coincided with suppressed fluxes. Particularly cold years within a regime, such as 1964, 1971, 1980, and 1984, are usually accompanied by enhanced net heat fluxes. There also seems to be some multi-year memory in the system. The winter of 1976 was very cold even though the net heat fluxes were moderate; this may be due to the cumulative effects of the cold winters and enhanced heat fluxes over the preceding 5 years. Similarly, the extreme fluxes of the winter of 1984 were accompanied by only a modest mean surface temperature anomaly, perhaps because it followed a prolonged warm period. As noted in the time series of anomalous mean temperature, no readily discernible long-term trends are present in the wind stress or heat fluxes.

Another important process during the cool season is the wind forcing of the large-scale upper ocean circulation of the Bering Sea. Two separate aspects of this wind forcing for the entire cool season (September through May) are presented in the bottom panel of Fig. 5. The first

---

[1]The climatological mean net surface heat flux is -153 W m^{-2}. The winter season averages are always negative, implying the atmosphere is always cooling the ocean, for the season as a whole. Therefore, negative anomalies imply enhanced cooling, and positive anomalies imply suppressed cooling.

is the wind stress curl evaluated over the eastern portion of the Bering Sea basin (55°N, 175°W). The wind stress curl measures the atmospheric forcing of the counter-clockwise gyre circulation within the Bering basin (Bond et al., 1994); the actual flow associated with this circulation tends to be concentrated along the bathymetry, and may ultimately relate to cross-shelf exchanges. Notable variations in the anomalous wind stress curl (solid line) include positive anomalies from the late 1970s through the late 1980s (coincident with a period of an enhanced Aleutian Low), and a weak overall positive trend, with the exception of the winters of 1996–97.

The second aspect of the wind forcing is the component of the surface wind stress evaluated along the Aleutian peninsula at 53°N, 173°W (Fig. 2). This parameter measures the direct wind forcing of the Aleutian North Slope Current (positive values signify winds from the southwest) and perhaps also the flow onto the southern end of the shelf. The anomalous along-peninsula wind stress (dotted line) correlates well with the curl but does not appear to have any systematic long-term trend. The large changes in both quantities between the winters of 1997 and 1998 provide an opportunity to gauge whether these parameters have any tangible effects on the circulation of the Bering Sea. This issue is pursued in the following section.

b. Spring and Summer

The interannual variability of the conditions over the middle shelf during the warm season is summarized in Fig. 6. The top panel of Fig. 6 shows the anomalous SST on August 1 (solid line) and the mean SST tendency for May through July (dotted line).[2] Both parameters respond to the local atmospheric forcing, but the August SST is also influenced by conditions at the end of the previous winter. Both time series show a upward trend over the last 40 years. The SST tendencies in the 1990s were roughly 1°C/100 days greater than they were in the 1960s; similarly, the August SST anomalies increase by roughly 1°C over the same period. The interannual variability in the seasonal mean SST tendencies is greater in the second half of the

[2]The SST tendency is plotted in terms of its actual rather than its anomalous values. The mid-point of the y-axis is its 40-year mean, and so values above (below) the zero anomaly line for the August SST may be interpreted as positive (negative) anomalies.

record.

These temperature records can be compared with the surface heating. For the season as a whole (mid-May through July), the mean values of each term comprising the net surface heat flux, and the standard deviations in these seasonal means, are itemized in Table 1. Here we focus on the term most responsible for the variability in the heating, the downward shortwave radiative flux, and a term responsible for much of the long-term trend in the heating, the latent heat flux. Figure 6 (middle panel) shows the 40-year time series for these two processes at Mooring 2 during the period of greatest warming (mid-May through July). The anomalous downward shortwave radiation (solid line) features large (10–20 W m^{-2}) interannual variations which are due to fluctuations in seasonally averaged low cloud coverage. Notable recent anomalies include the relatively sunny and cloudy summers of 1997 and 1998, respectively. There has been a slight trend towards greater solar heating, amounting to an increase of roughly 5 W m^{-2} over the period of record. The correlation between the seasonal mean downward shortwave flux and the SST tendencies is 0.4 (significant at the 99% confidence level). The time series of anomalous latent heat fluxes (dotted line) shows much less interannual variability and a more systematic trend towards lesser negative fluxes, i.e., less cooling of the ocean. Again, the difference in the latent heat flux is roughly 5 W m^{-2} over the period of record. The decrease in latent heat fluxes is largely attributable to a decrease in surface wind speeds rather than a decrease in the air-sea humidity difference. An increase of 10 W m^{-2} in the atmospheric heating of the ocean, when applied over 100 days, and distributed over 20 m (a typical upper mixed layer depth over the middle shelf), would cause an SST warming of ~1°C. This increase is consistent with the differences observed in the mean SST and SST tendency (Fig. 6).

In addition to the heating mechanisms described above, the wind forcing also strongly influences conditions over the shelf during the warm season. The bottom panel of Fig. 6 displays the seasonal mean wind mixing as well as the along-shelf wind stress evaluated at the shelf break along the eastern boundary of the Bering basin near the mouth of Pribilof Canyon (56°N, 169°W). The time series of anomalous wind mixing for June–July (solid line) shows that early

summer was relatively stormy in the early 1970s and calm throughout the 1980s. Generally light wind mixing prevailed in the 1990s, except for in 1993 and 1996. The along-shelf wind stress is important because of its influence on the exchange of water between the basin and shelf. These exchanges can occur directly, via Ekman drift, or indirectly, through the wind's forcing of the Bering Slope current, which itself may be linked to eddy activity along the shelf break. The time series of the anomalous along-shelf stress for May–July (dotted line) indicates a tendency for positive values (i.e., towards the west-northwest) over the last two decades, with a particularly prominent positive anomaly in 1997. This implies that the atmosphere has been contributing towards greater along-shelf transports in the latter half of the record.

5. Discussion

The daily time series presented for the winters of 1995–99 indicate that the weather events that give rise to sea ice over the shelf last roughly 4–12 days. This timescale is substantially longer than the 1–3-day scale that typifies individual weather disturbances, i.e., cyclones or anticyclones. This implies that persistent weather anomalies, typically accompanied by "families" of disturbances, are required for substantial advances or retreats in sea ice.

The characteristics of the forcing that produces sea ice exhibits some change over the course of the winter season. Early sea ice, i.e., in January and early February, requires strongly anomalous heat fluxes for cooling since ocean temperatures are climatologically too warm to support ice. Later in the winter, ocean temperatures are colder and the ice edge is often just to the north or northeast, and moderate off-shelf winds can be sufficient to bring ice to the location of Mooring 2.

The low correlation ($R \sim 0.3$) between seasonal mean winds and ice extent (Niebauer et al., 1999) can be explained by the highly episodic nature of the sea ice forcing and the importance of the preconditioning or cooling of the water column by the surface heat fluxes. The winds and fluxes during individual winters are moderately correlated ($R \sim 0.5$), but these parameters also exhibit substantial independence. Similar winds can occur with two entirely

different air masses. Based on our synoptic experience, the heat flux into an arctic air mass (generally associated with anticyclones that have developed over high-latitude continental or pack-ice regions) is much greater than the flux into a warmer, moist maritime air mass (often associated with cyclones). In essence, a shift in the frequency distribution of these synoptic weather events accounts for the differences in seasonal mean forcing of sea ice. Shifts in this frequency distribution will be reflected in the magnitude and position of the seasonal mean Aleutian low. As illustrated by Overland et al. (1999), the Aleutian low was relatively weak during the cold winters of the early 1970s in the Bering Sea, and was relatively strong during the warm winters of the late 1970s through much of the 1980s.

The seasonal means summarized in section 4a and depicted in Fig. 5 indicate that the recent short-term climate changes in the Bering Sea during winter are of a different character than for the North Pacific as a whole. The Bering Sea exhibits much of its variability on time scales of roughly a decade, while the North Pacific appears to have much of its variability on multi-decadal timescales in association with the PDO. This result is consistent with Overland et al. (1999) who point out the higher-frequency variability for the Aleutian Low than for the PDO. The Bering Sea is influenced significantly by a number of climate modes (e.g., also the Arctic Oscillation or AO; Thompson and Wallace, 1998), rather than dominated by a single mode.

The Aleutian North Slope Current (ANSC) is an eastward current along the north side of the Aleutian islands between roughly 170°E and 166°W (Stabeno et al., 2001a) that represents an important component of the circulation of the southeast Bering Sea. The ANSC is fed largely by water flowing through the passes in the Aleutian Island chain. We use the reanalysis data set and transports estimated from multiple hydrographic sections in 1997 and 1998 to assess whether the ANSC is sensitive to wind forcing on seasonal timescales. The mean transports of the ANSC during 1997 and 1998 were approximately 6.0 and 2.1 Sverdrups, respectively (R. Reed, personal communication). Figure 5 (bottom panel) shows that the anomalous along-peninsula wind stress was strongly negative (from the east–northeast) in 1997 and strongly positive (from the west–southwest) in 1998. For these 2 years, the difference in the sense of these wind stress

anomalies along the peninsula was opposite to the difference in the transport of the ANSC.

We have an explanation for this seemingly puzzling result. The source of the inflow into the Aleutian passes is largely the Alaskan Stream, the current along the shelf break on the south side of the Alaska Peninsula and the Aleutian islands. Processes that impact the Alaskan Stream should also impact the ANSC. In particular, during extended (weekly and longer) periods of negative along-peninsula wind stress anomalies such as in 1997, Ekman drift towards the north will tend to press the Alaskan Stream against the shelf break. Under these conditions, a relatively large portion of the flow associated with the Alaskan Stream would follow the isobaths leading to the Aleutian passes, contributing toward enhanced inflows into the ANSC. Conversely, we expect that positive along-peninsula wind anomalies such as in 1998, would result in the Alaskan Stream being farther offshore than usual, with reduced inflows into the ANSC.

The evidence at hand is more suggestive than definitive, but it does appear that the ANSC responds more to the forcing of the flow through the Aleutian passes than to the "set-up" of sea level associated with Ekman drift on the north side of the Aleutians. Because of the probable importance of this current to the circulation in the southern Bering Sea, it would be valuable to gain more complete understanding of its causes.

Our analysis of spring and summer over the Bering Sea shelf focused on the intraseasonal to interannual fluctuations in SST tendency, and its links to variations in the local heating and wind forcing. Low cloud cover is nearly ubiquitous over the Bering sea during the warm season, so a few episodes of relatively clear skies can dominate the seasonal mean insolation. The daily time series presented in Figs. 4a–e indicate that reduced shortwave fluxes are generally accompanied by enhanced wind mixing. This implies that the clouds with more vigorous disturbances are thicker or more extensive (i.e., they reflect or absorb more solar radiation) than the clouds present under calmer conditions. This result is consistent with the climatology of Norris (1998), which showed that the low clouds in the Bering Sea are associated most frequently with weak warm air advection in the eastern sector of cyclonic weather disturbances.

The synoptic weather environment of the Bering Sea is fairly active even during the

warm season, so the low cloud coverage is more closely related to fluctuations in the large-scale atmospheric circulation than in local boundary conditions. The SST does have important feedbacks on atmospheric boundary layer structure and stratus cloud decks in the eastern portions of the subtropical oceans (Ronca and Battisti, 1997), but in high-latitude oceans such as the Bering Sea, the SST predominately responds to the variations in the clouds rather than causes them.

The long-term warming trend in warm season SST over the Bering Sea shelf is consistent with the results of Norris et al. (1998). The trend in the principal component of their leading EOF of summertime North Pacific SST implies warming for the Bering Sea. That a long-term warming trend can be identified for the Bering Sea in summer, but not in winter, is not a surprise. Considering air temperatures for the entire Northern Hemisphere poleward of 40°N, Wallace et al. (1996) found that the interannual variability obscures interdecadal trends during winter much more than during summer. It bears noting that the magnitude of the trend in the summertime warming over the Bering Sea shelf is on the order of 5–10 times greater than that for the northern oceans as a whole.

Norris et al. (1998) found negative correlations between SST and cloud cover over the Bering Sea. The large-scale circulation anomalies or climate mode variations accompanying these changes in summertime SST are poorly understood. Overland et al. (2001a) showed that the two leading atmospheric modes during spring and summer, the North Pacific and East Pacific patterns, exhibit substantial variability on decadal time scales. But it is unknown whether these modes represent just intrinsic, and perhaps unpredictable variability in the Northern Hemisphere circulation during the warm season, or whether they are subject to external effects such as ENSO, or North Pacific SST. The degree to which these modes are correlated with local air-sea interactions over the shelf is examined in a companion paper in this volume (Overland et al., 2001b).

6. Summary

The results of our analyses of the daily atmospheric forcing of sea ice in winter, and SST from spring into summer, for the period 1995–99 is summarized in Table 2. Daily time series are required to adequately resolve the weather events that are responsible for much of the variability in the forcing. As indicated in Table 2, the 5-year period of 1995 through 1999 included a representative sample of the conditions that can occur over the Bering Sea shelf. We suspect that the variations documented here can account directly for some of the year-to-year differences in the marine ecosystem (e.g., the timing and magnitude of the spring bloom, Hunt et al., 2001, this volume; the differences in zooplankton species concentrations, Napp et al., 2001, this volume) that were found for the same period.

Seasonal averages of the local atmospheric forcing of the Bering Sea shelf during the winter and spring/summer have been compiled for the last 40 years (Figs. 5 and 6). Winter conditions featured cold, off-shelf (northeasterly) winds in the early to middle 1970s and sudden reversal to relative warmth in the late 1970s to early 1980s, but little if any systematic trend over the 40-year period considered here. During the spring and early summer, a weak trend, on top of considerable interannual variability, is discernible in the atmospheric forcing and physical oceanographic response. Compared to the 1960s, the climate of the 1990s includes about 10 W m^{-2} more atmospheric heating from mid-May through July. Downward shortwave radiation and surface latent heat fluxes contributed comparably to this increase. As a result, the SST warmed ~1°C more in the spring and early summer of the 1990s than in previous decades.

Acknowledgments

We thank Jim Overland, Ron Reed, and Phyllis Stabeno for useful discussions. We appreciate the constructive reviews by Nate Mantua and an anonymous reviewer. This publication was supported by the Joint Institute for the Study of the Atmosphere and Ocean (JISAO) under NOAA Cooperative Agreement #NA67RJO155, Contribution #788. PMEL Contribution #2257.

References

Adams, J.M., Bond, N.A., J.E. Overland, 2000. Regional variability of the Arctic heat budget in fall and winter. Journal of Climate 13, 3500–3510.

Bond, N.A., Overland, J.E., Turet, P., 1994. Spatial and temporal characteristics of the wind forcing of the Bering Sea. Journal of Climate 7, 1119–1130.

Graham, N.E., 1994. Decadal-scale climate variability in the 1970s and 1980s: Observations and model results. Climate Dynamics 10, 135–162.

Hunt, G.L., Stabeno, P.J., Walters, G., Sinclair, E., Brodeur, R.D., Napp, J.M., Bond, N.A., 2001. The Eastern Bering Sea: Three decades of change. Deep-Sea Research II: Topical Studies in Oceanography (this volume).

Kachel, N.B., Salo, S.A., Schumacher, J.D., Stabeno, P.J., Whitledge, T.E., 2001. Characteristics of the inner front of the southeastern Bering Sea. Deep-Sea Research II: Topical Studies in Oceanography (this volume).

Kalnay, E., et al., 1996. The NCEP/NCAR 40-year reanalysis project. Bulletin of the American Meteorological Society 77, 437–471.

Mantua, N.J., Hare, S.R., Zhang, Y., Wallace, J.M., Francis, R.C., 1997. A Pacific interdecadal climate oscillation with impacts on salmon production. Bulletin of the American Meteorological Society 78, 1069–1079.

Napp, J.M., Baier, C.T., Coyle, K.O., Brodeur, R.D., Shiga, N., Mier, K., 2001. Interannual and Decadal Variability in Zooplankton Communities of the Southeast Bering Sea Shelf. Deep-Sea Research II: Topical Studies in Oceanography (this volume).

Niebauer, H.J., Bond, N.A., Yakunin, L.P., Plotnikov, V.V., 1998. On the climatology and ice of the Bering Sea. In "Dynamics of the Bering Sea", T.R. Loughlin and K. Ohtani (eds.), North Pacific Marine Science Organization (PICES), University of Alaska Sea Grant, AK-SG-99-03, 29–59.

Norris, J.R., 1998. Low cloud type over the ocean from surface observations. Part II: Geographical and seasonal variations. Journal of Climate 11, 383–403.

Norris, J.R., Zhang, Y., Wallace, J.M., 1998. Role of low clouds in summertime atmosphere-ocean interactions over the North Pacific. Journal of Climate 11, 2482–2490.

Overland, J.E., Adams, J.M., Bond, N.A., 1999. Decadal variability of the Aleutian Low and its relation to high-latitude circulation. Journal of Climate 12, 1542–1548.

Overland, J.E., Bond, N.A., Adams, J.M., 2001a. North Pacific atmospheric and SST anomalies in 1997: Links to ENSO? Fisheries Oceanography (in press).

Overland, J.E., Bond, N.A., Adams, J.M., 2001b. Downscaling atmospheric teleconnections for the spring transition in the Bering Sea. Deep-Sea Research II: Topical Studies in Oceanography (this volume).

Pease, C.H., 1980. Eastern Bering sea ice processes. Monthly Weather Review 108, 2015–2023.

Reed, R.K., Stabeno, P.J., 2001. Surface heat fluxes and subsurface heat content at a site over the southeastern Bering Sea shelf, May–June 1996. Deep-Sea Research II: Topical Studies in Oceanography (this volume).

Reynolds, R.W., Smith, T.M., 1994. Improved global sea surface temperature analyses using optimum interpolation. Journal of Climate 7, 929–948.

Stabeno, P.J., Bond, N.A., Kachel, N.B., Salo, S.A., Schumacher, J.D., 2001a. On the temporal variability of the physical environment over the southeastern Bering Sea. Fisheries Oceanography (in press).

Stabeno, P.J., Kachel, N.B., Sullivan, M., Whitledge, T.E., 2001b. Variability along the 70-m isobath of the Southeast Bering Sea. Deep-Sea Research II: Topical Studies in Oceanography (this volume).

Thompson, D.W.J., Wallace, J.M., 1998. The Arctic Oscillation signature in the wintertime geoptential height and temperature fields. Geophysical Research Letters 25, 1297–1300.

Trenberth, K.E., Hurrell, J.W., 1994. Decadal atmosphere-ocean variations in the Pacific. Climate Dynamics 9, 303–319.

Wallace, J.M., Zhang, Y., Bajuk, L., 1996. Interpretation of interdecadal trends in Northern Hemisphere surface air temperature. Journal of Climate 9, 249–259.

Wyllie-Echeverria, T., Wooster, W.S., 1998. Year to year variation in Bering Sea ice cover and some consequences for fish distribution. Fisheries Oceanography 7, 159–170.

Yang, S.-K., Hou, Y.-T., Miller, A.J., Campana, K.A., 1999. Evaluation of the Earth Radiation Budget in NCEP-NCAR Reanalysis with ERBE. Journal of Climate 12, 477–493.

Zhang, Y., Wallace, J.M., Battisti, D.S., 1997. ENSO-like interdecadal variability: 1900–93. Journal of Climate 10, 1004–1020.

Table 1

Surface heat fluxes in summer: summary statistics

Heat Flux Term	Seasonal Mean (W/m^2)	Standard Deviation (W/m^2)
Sensible Heat	6.6	2.5
Latent Heat	–6.0	3.4
Downward Shortwave	241.7	9.6
Upward Shortwave	–38.1	1.4
Downward Longwave	299.2	3.4
Upward Longwave	–344.3	3.5
Net	159.1	8.3

Table 2

Highlights of 1995–1999 over the Bering Sea shelf

Year	Winter	Summer
1995	Heavy Ice, Off-shelf Winds	Calm and Sunny Early
1996	Little Ice, On-shelf Winds	Frequent Moderate Storms
1997	Near-Normal Forcing & Ice	Calm and Sunny, El Niño
1998	Cool Early but an Early Thaw	Warm Early, Late Storms
1999	Warm Early, Heavy Ice Late	Weak Winds, Cool Mid-Summer

Figure Captions

Fig. 1. Daily averages of meridional winds (m s^{-1}, top two panels) and downward shortwave radiation (W m^{-2}, bottom two panels) observed at Mooring 2 (57°N, 164°W) and from the NCEP/NCAR Reanalysis at Mooring 2 for spring and summer of 1996 and 1999. The observations and the reanalysis are indicated with solid and dotted lines, respectively.

Fig. 2. Map of study area. The location of Mooring 2 (where many of the air-sea interaction parameters are evaluated) is labeled M2. The locations where the net surface heat flux, the wind stress curl, the along-peninsula wind stress, and the along-shelf wind stress are labeled HF, WC, AP, and AS, respectively. The light dashed line indicates the 1000-m isobath. The maximum ice extents for the winters 1995 through 1999 (based on thrice-weekly ice charts from the Anchorage, AK, National Weather Service Forecast Office) are also shown.

Fig. 3a. Daily values of surface temperature at 57°N, 164°W (°C, top panel), net surface heat flux at 56°N, 172°W (W m^{-2}, middle panel) and cross-shelf wind stress at 57°N, 164°W (N m^{-2}, bottom panel) from the NCEP/NCAR Reanalysis for December 1994–April 1995. The dotted lines represent climatological means (1959–1999).

Fig. 3b. As in Fig. 2a, but for December 1995–April 1996.

Fig. 3c. As in Fig. 2a, but for December 1996–April 1997.

Fig. 3d. As in Fig. 2a, but for December 1997–April 1998.

Fig. 3e. As in Fig. 2a, but for December 1998–April 1999.

Fig. 4a. Daily values of sea surface temperature tendency (°C/10 days, top panel), wind mixing (u^{*3}) ($m^3 s^{-3}$, middle panel), and downward shortwave flux ($W m^{-2}$, bottom panel) from the NCEP/NCAR Reanalysis at Mooring 2 (57°N, 164°W) for May–September 1995. The dotted lines represent climatological means (1959–1999).

Fig. 4b. As in Fig. 3a, but for 1996.

Fig. 4c. As in Fig. 3a, but for 1997.

Fig. 4d. As in Fig. 3a, but for 1998.

Fig. 4e. As in Fig. 3a, but for 1999.

Fig. 5. Winter season average anomalies for 1959–1999. Top: surface temperature at 57°N, 164°W (solid line, °C). Middle: cross-shelf wind stress at 57°N, 164°W (solid line, $N m^{-2}$) and net surface heat flux at 56°N, 172°W (dotted line, $W m^{-2}$). Bottom; wind stress curl at 55°N, 175°W (solid line, $N m^{-3} \times 10^7$) and along-peninsula wind stress at 53°N, 173°W (dotted line, $N m^{-2}$).

Fig. 6. Summer season averages for 1959–1999. Top: SST tendency (solid line, °C/100d) and SST anomaly on 1 August (dotted line, °C), both at 57°N, 164°W. The zero anomaly line for the SST also represents the value of the mean SST tendency. Middle; downward shortwave radiative heat flux anomaly (solid line, $W m^{-2}$) and surface latent heat flux anomaly (dotted line, $W m^{-2}$), both at 57°N, 164°W. Bottom: wind mixing anomaly at 57°N, 164°W (solid line, $m^3 s^{-3} \times 100$) and along-shelf wind stress anomaly at 56°N, 169°W (dotted line, $N m^{-2}$).

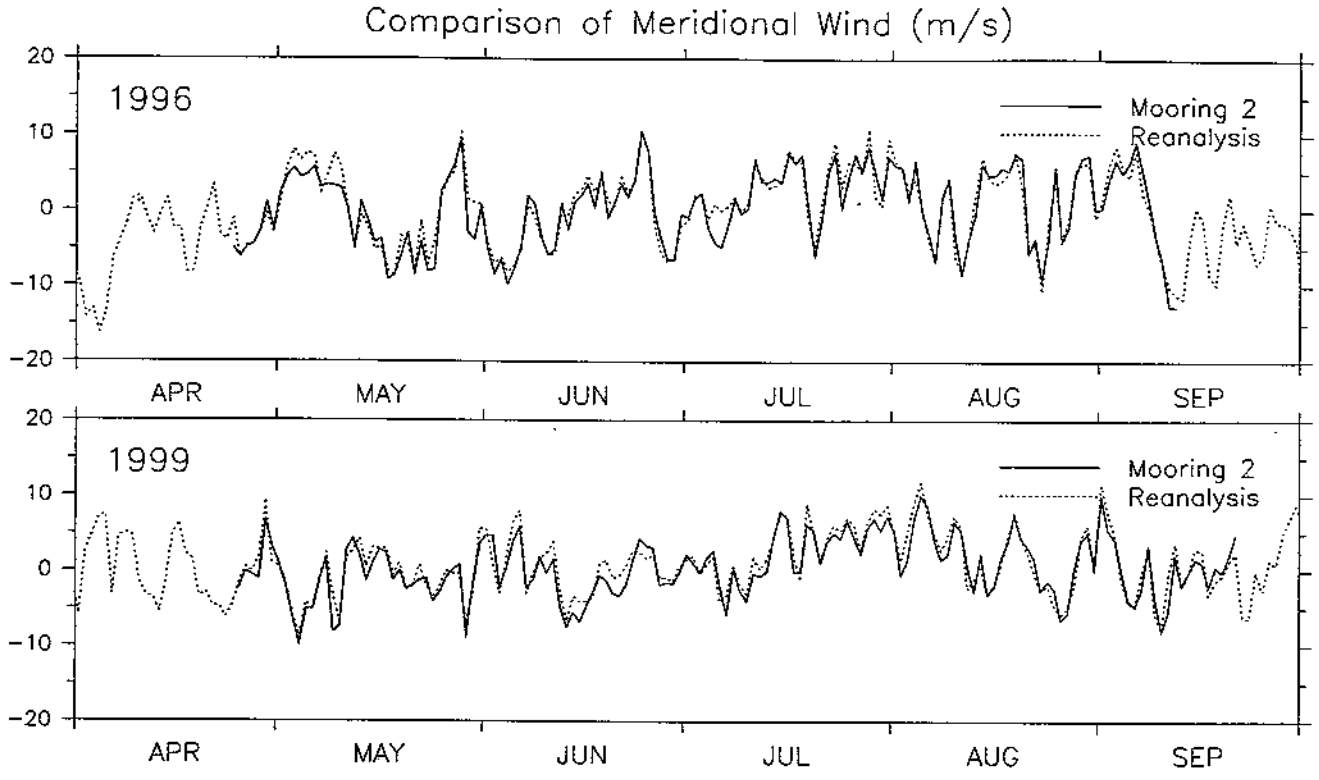
Comparison of Meridional Wind (m/s)
1996
Mooring 2
Reanalysis
20
10
0
−10
−20
APR
MAY
JUN
JUL
AUG
SEP
1999
Mooring 2
Reanalysis
20
10
0
−10
−20
APR
MAY
JUN
JUL
AUG
SEP

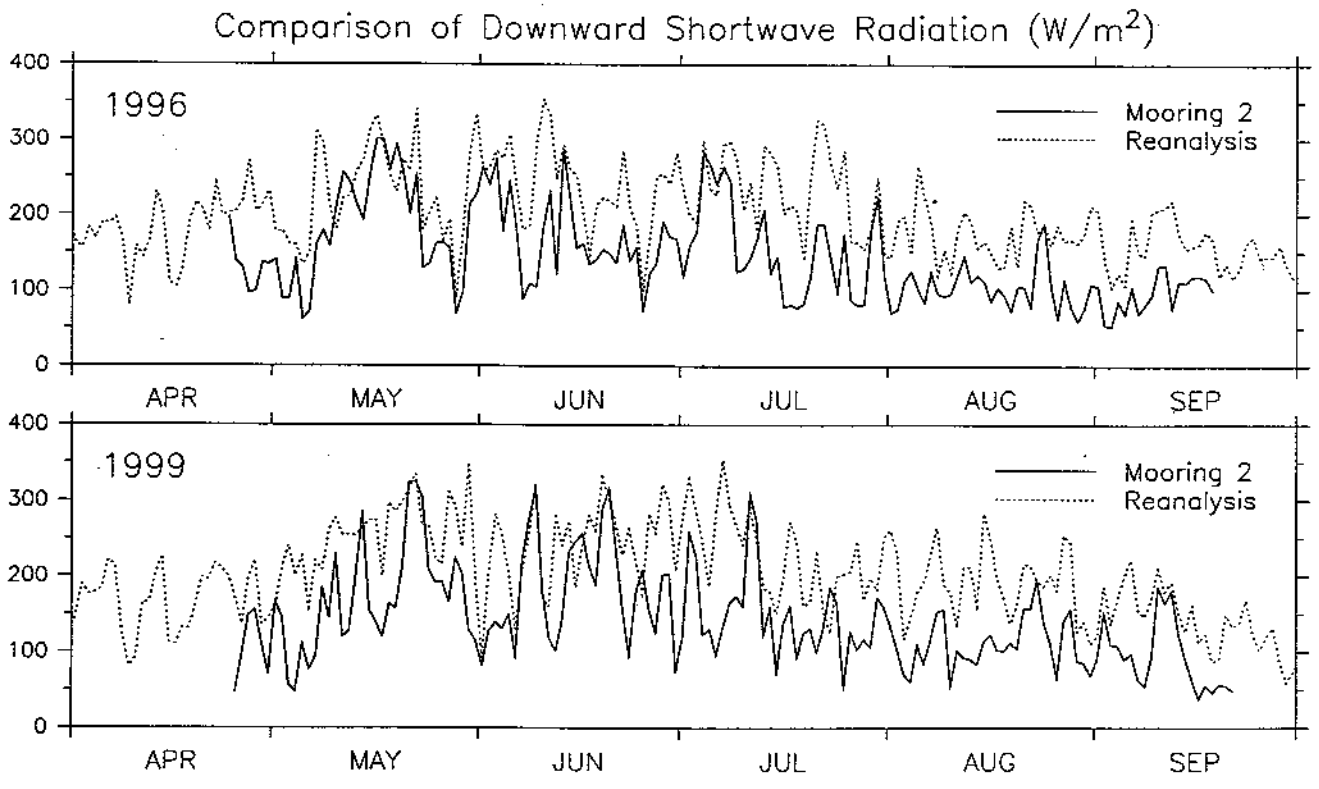
Comparison of Downward Shortwave Radiation (W/m2)
1996
Mooring 2
Reanalysis
400
300
200
100
0
APR
MAY
JUN
JUL
AUG
SEP
1999
Mooring 2
Reanalysis
400
300
200
100
0
APR
MAY
JUN
JUL
AUG
SEP

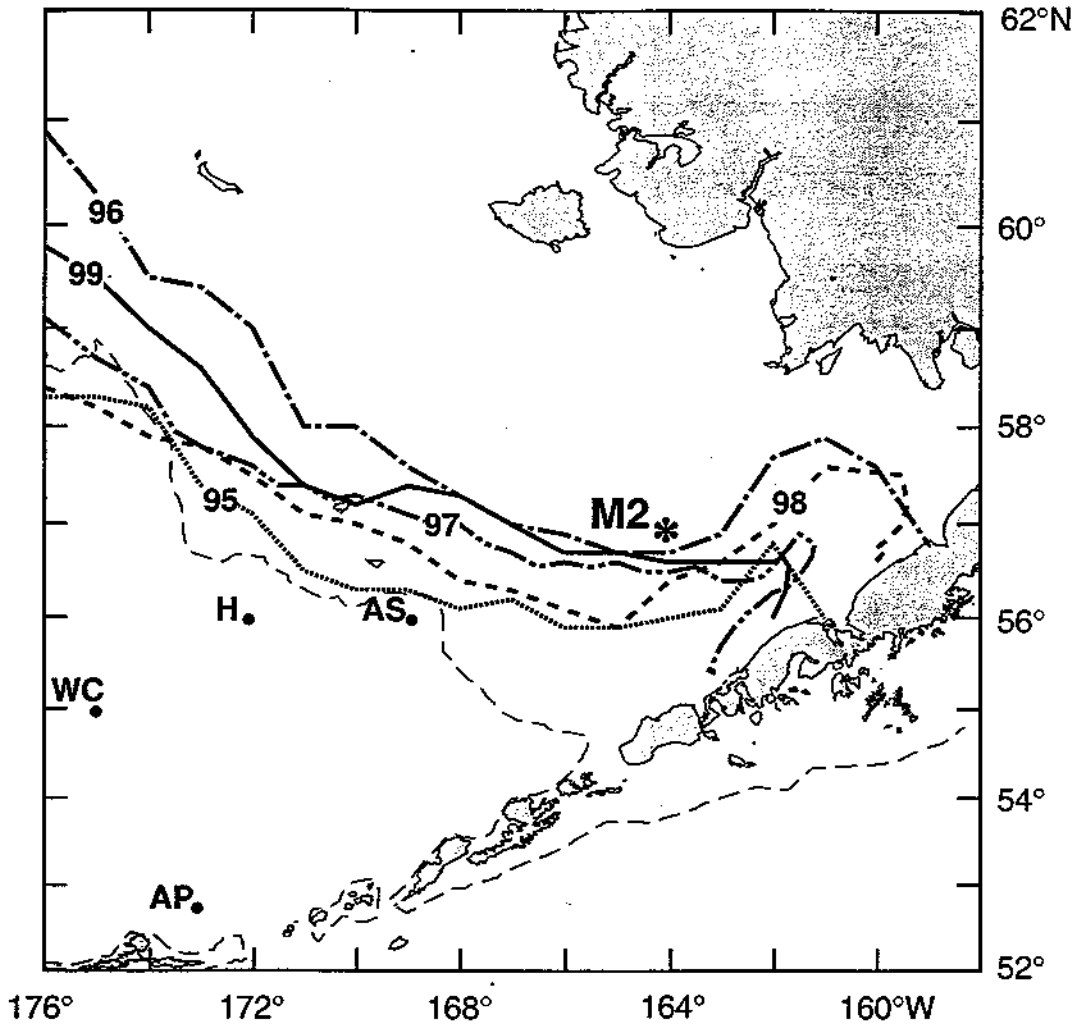
62°N
60°
58°
56°
54°
52°
176°
172°
168°
164°
160°W
96
99
95
97
98
M2
H
AS
WC
AP

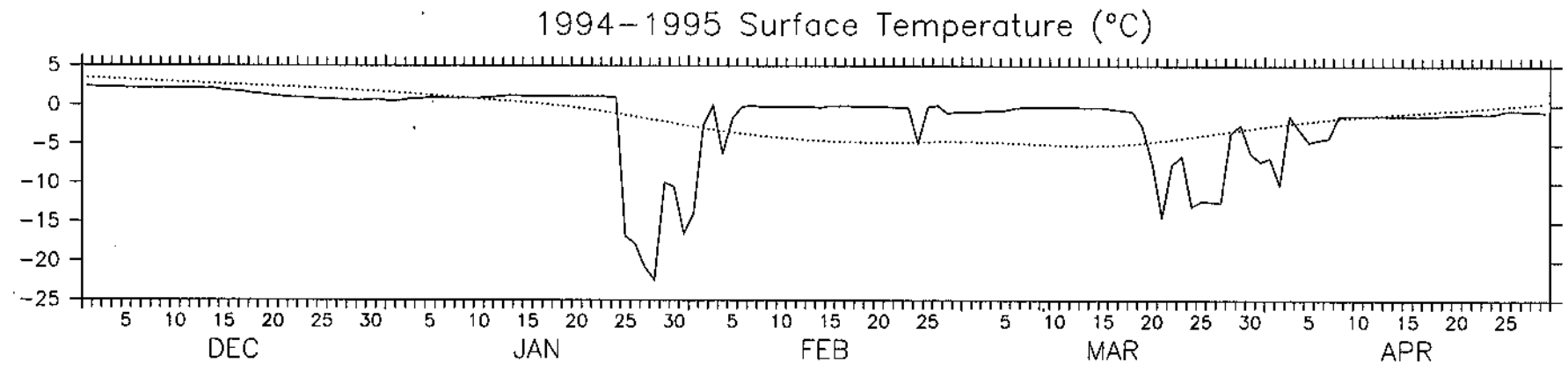
1994–1995 Surface Temperature (°C)
5
0
−5
−10
−15
−20
−25
5 10 15 20 25 30 5 10 15 20 25 30 5 10 15 20 25 5 10 15 20 25 30 5 10 15 20 25
DEC
JAN
FEB
MAR
APR

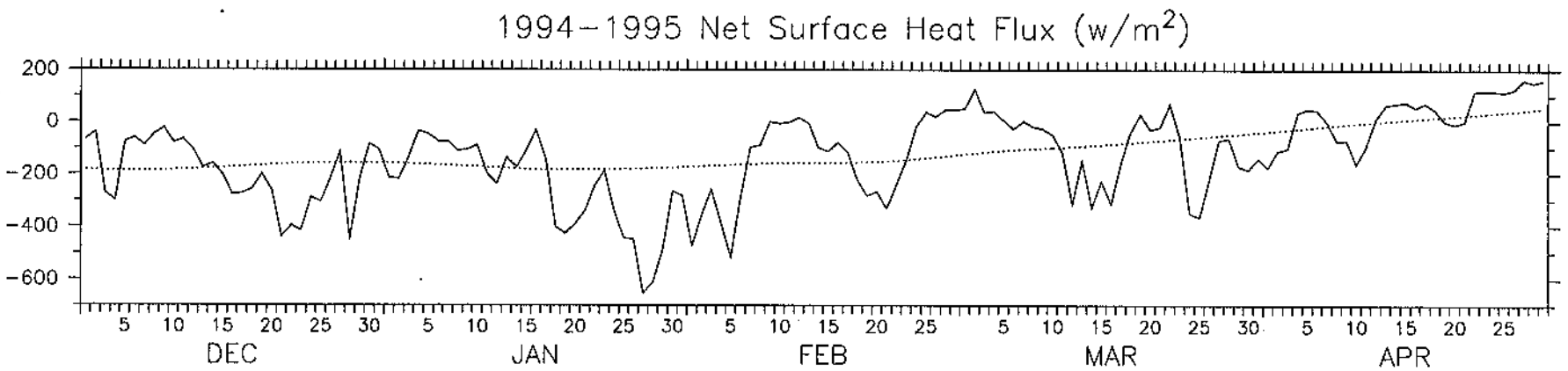
1994–1995 Net Surface Heat Flux (w/m^2)
200
0
−200
−400
−600
5 10 15 20 25 30 5 10 15 20 25 30 5 10 15 20 25 5 10 15 20 25 30 5 10 15 20 25
DEC
JAN
FEB
MAR
APR

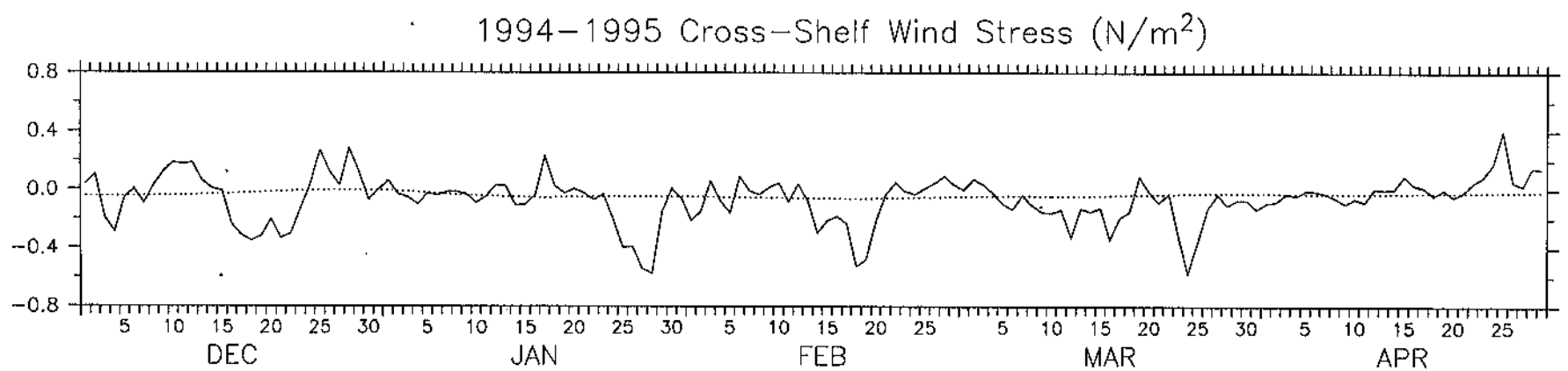
1994–1995 Cross–Shelf Wind Stress (N/m^2)
0.8
0.4
0.0
−0.4
−0.8
5 10 15 20 25 30 5 10 15 20 25 30 5 10 15 20 25 5 10 15 20 25 30 5 10 15 20 25
DEC
JAN
FEB
MAR
APR

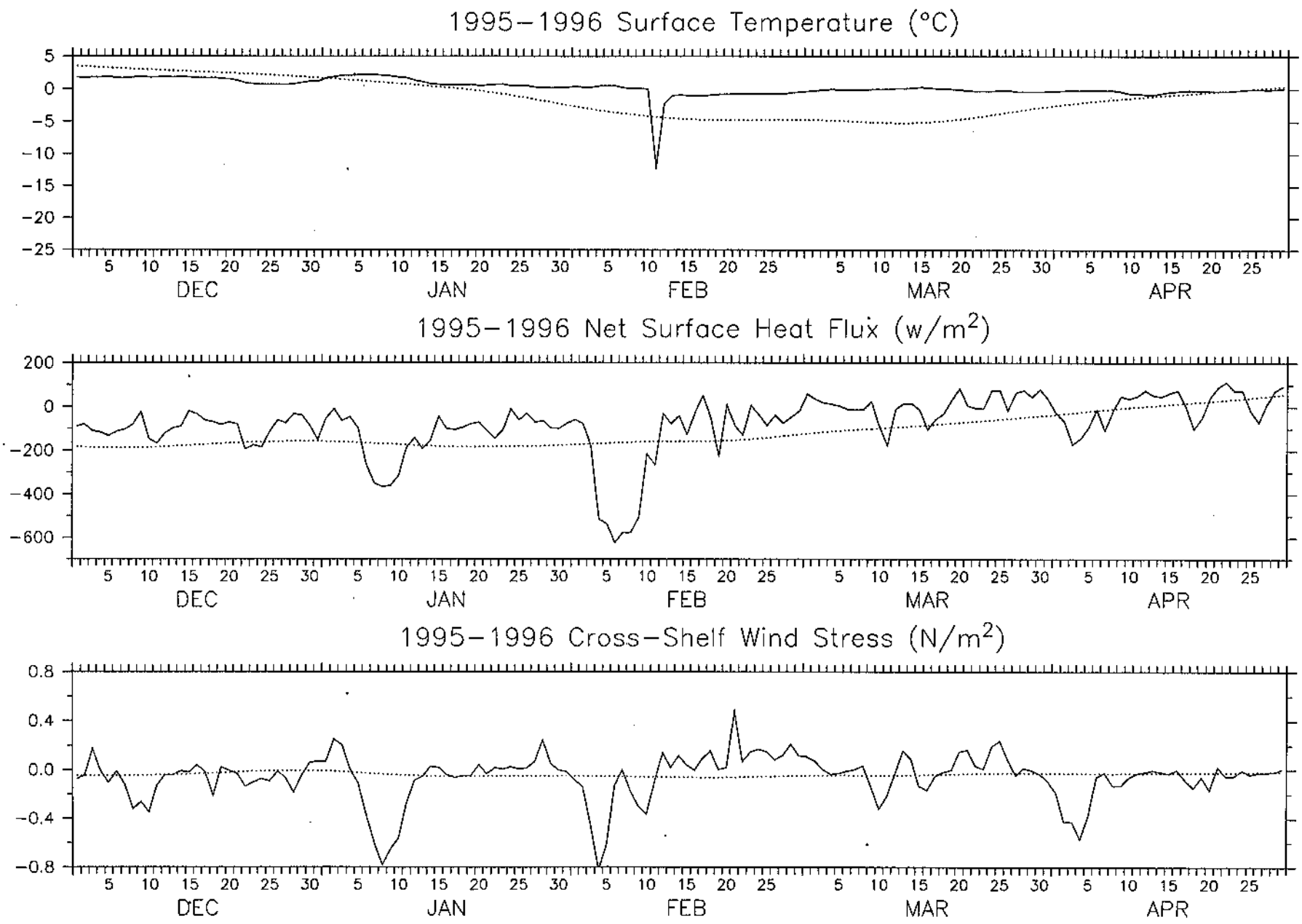
1995–1996 Surface Temperature (°C)
5
0
−5
−10
−15
−20
−25
5 10 15 20 25 30 5 10 15 20 25 30 5 10 15 20 25 5 10 15 20 25 30 5 10 15 20 25
DEC
JAN
FEB
MAR
APR
1995–1996 Net Surface Heat Flux (w/m2)
200
0
−200
−400
−600
5 10 15 20 25 30 5 10 15 20 25 30 5 10 15 20 25 5 10 15 20 25 30 5 10 15 20 25
DEC
JAN
FEB
MAR
APR
1995–1996 Cross–Shelf Wind Stress (N/m2)
0.8
0.4
0.0
−0.4
−0.8
5 10 15 20 25 30 5 10 15 20 25 30 5 10 15 20 25 5 10 15 20 25 30 5 10 15 20 25
DEC
JAN
FEB
MAR
APR

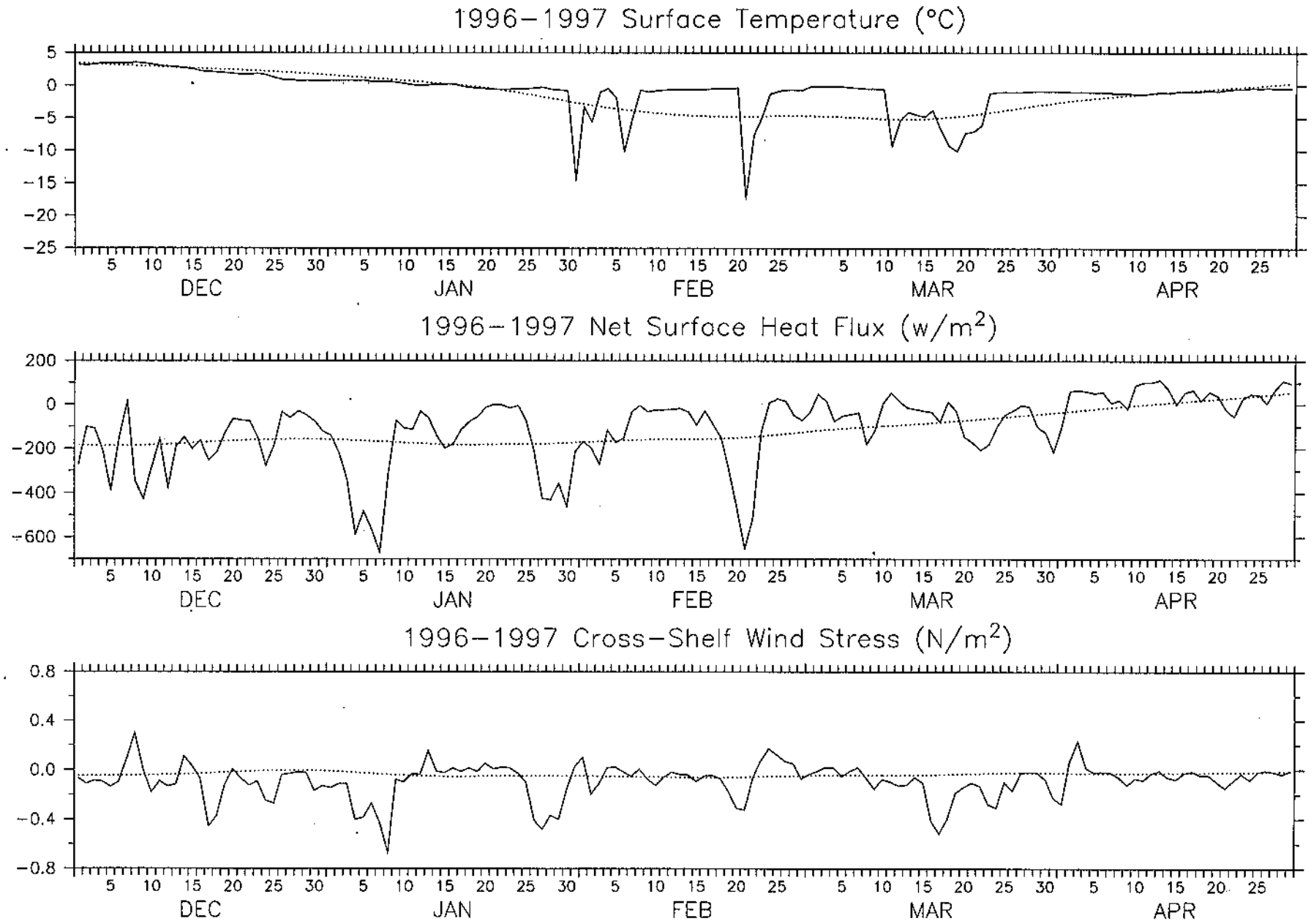
1996–1997 Surface Temperature (°C)
5
0
−5
−10
−15
−20
−25
5 10 15 20 25 30 5 10 15 20 25 30 5 10 15 20 25 5 10 15 20 25 30 5 10 15 20 25
DEC
JAN
FEB
MAR
APR
1996–1997 Net Surface Heat Flux (w/m2)
200
0
−200
−400
−600
5 10 15 20 25 30 5 10 15 20 25 30 5 10 15 20 25 5 10 15 20 25 30 5 10 15 20 25
DEC
JAN
FEB
MAR
APR
1996–1997 Cross–Shelf Wind Stress (N/m2)
0.8
0.4
0.0
−0.4
−0.8
5 10 15 20 25 30 5 10 15 20 25 30 5 10 15 20 25 5 10 15 20 25 30 5 10 15 20 25
DEC
JAN
FEB
MAR
APR

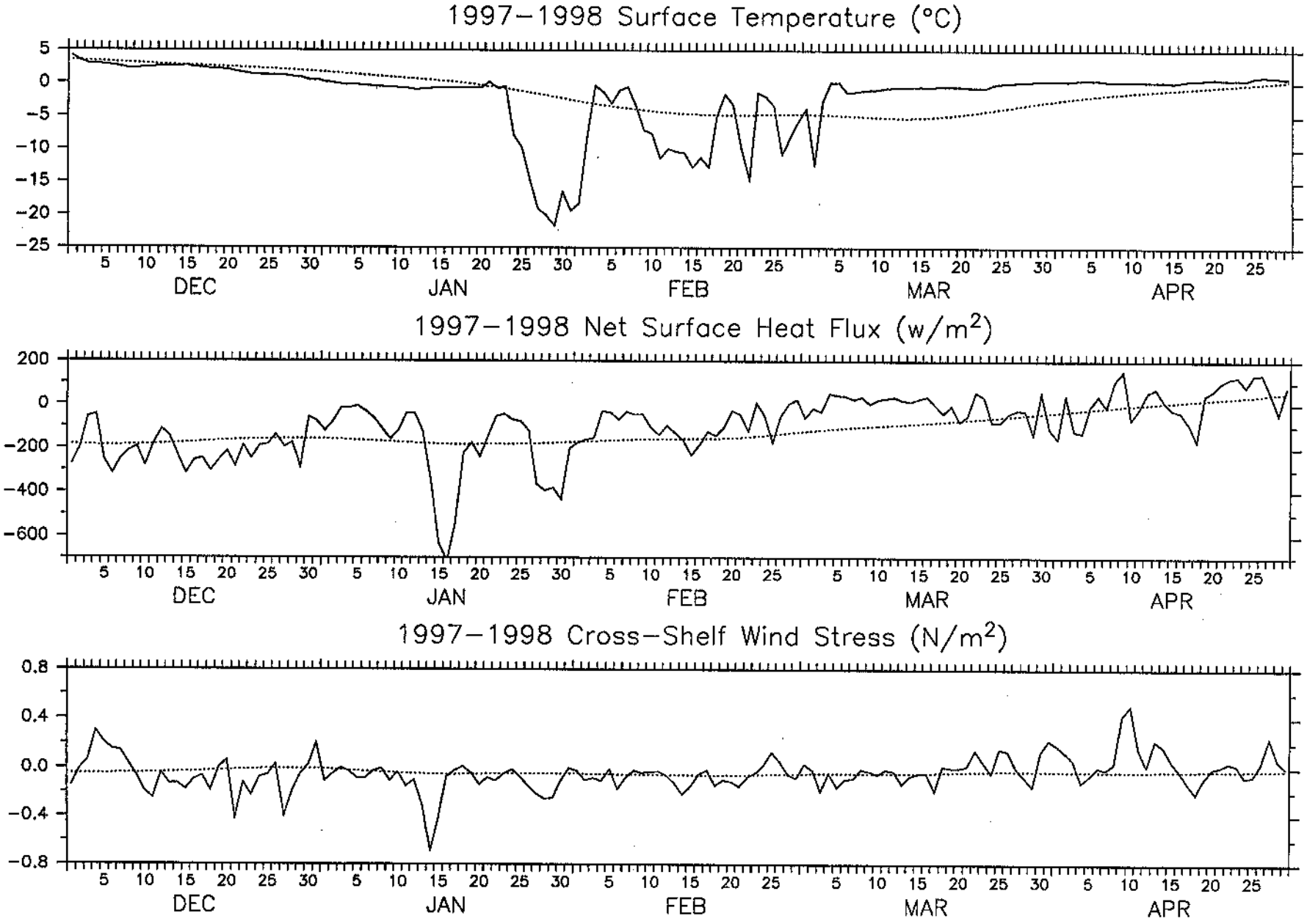
1997–1998 Surface Temperature (°C)
5
0
−5
−10
−15
−20
−25
5 10 15 20 25 30 5 10 15 20 25 30 5 10 15 20 25 5 10 15 20 25 30 5 10 15 20 25
DEC
JAN
FEB
MAR
APR
1997–1998 Net Surface Heat Flux (w/m²)
200
0
−200
−400
−600
5 10 15 20 25 30 5 10 15 20 25 30 5 10 15 20 25 5 10 15 20 25 30 5 10 15 20 25
DEC
JAN
FEB
MAR
APR
1997–1998 Cross–Shelf Wind Stress (N/m²)
0.8
0.4
0.0
−0.4
−0.8
5 10 15 20 25 30 5 10 15 20 25 30 5 10 15 20 25 5 10 15 20 25 30 5 10 15 20 25
DEC
JAN
FEB
MAR
APR

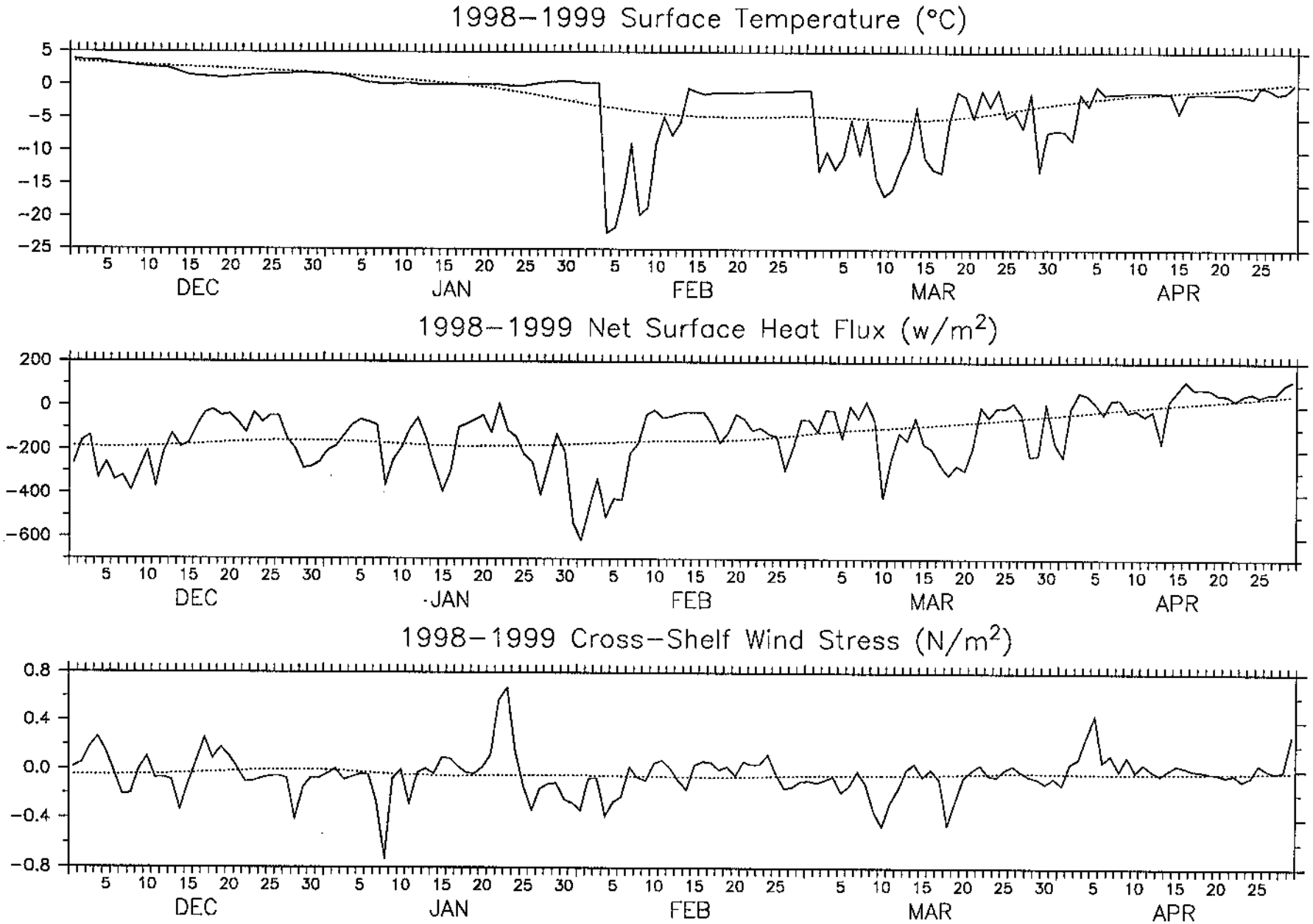
1998–1999 Surface Temperature (°C)
5
0
−5
−10
−15
−20
−25
5 10 15 20 25 30 5 10 15 20 25 30 5 10 15 20 25 5 10 15 20 25 30 5 10 15 20 25
DEC
JAN
FEB
MAR
APR
1998–1999 Net Surface Heat Flux (w/m2)
200
0
−200
−400
−600
5 10 15 20 25 30 5 10 15 20 25 30 5 10 15 20 25 5 10 15 20 25 30 5 10 15 20 25
DEC
JAN
FEB
MAR
APR
1998–1999 Cross–Shelf Wind Stress (N/m2)
0.8
0.4
0.0
−0.4
−0.8
5 10 15 20 25 30 5 10 15 20 25 30 5 10 15 20 25 5 10 15 20 25 30 5 10 15 20 25
DEC
JAN
FEB
MAR
APR

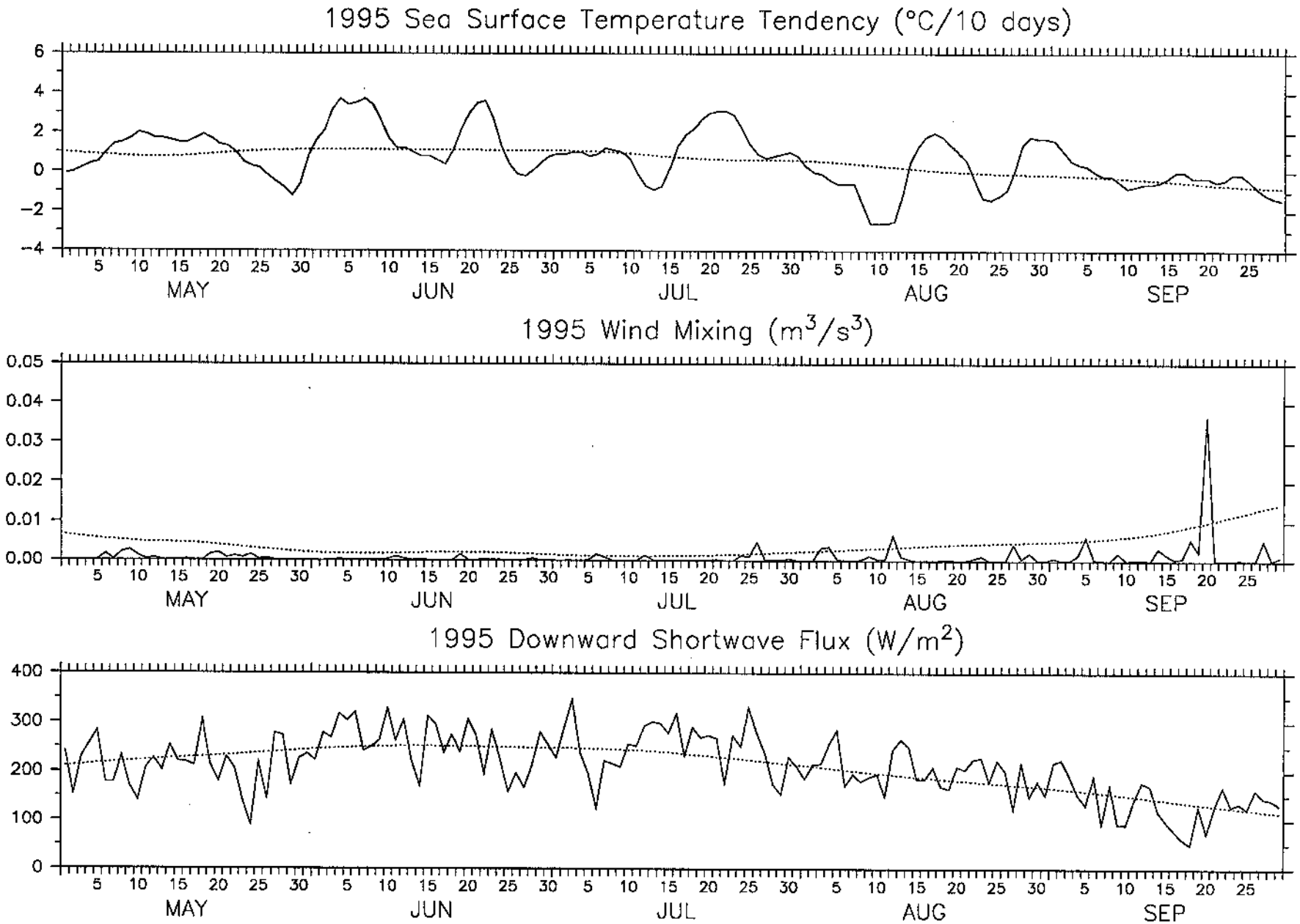
1995 Sea Surface Temperature Tendency (°C/10 days)
6
4
2
0
−2
−4
5 10 15 20 25 30 5 10 15 20 25 30 5 10 15 20 25 30 5 10 15 20 25 30 5 10 15 20 25
MAY
JUN
JUL
AUG
SEP
1995 Wind Mixing (m^3/s^3)
0.05
0.04
0.03
0.02
0.01
0.00
5 10 15 20 25 30 5 10 15 20 25 30 5 10 15 20 25 30 5 10 15 20 25 30 5 10 15 20 25
MAY
JUN
JUL
AUG
SEP
1995 Downward Shortwave Flux (W/m^2)
400
300
200
100
0
5 10 15 20 25 30 5 10 15 20 25 30 5 10 15 20 25 30 5 10 15 20 25 30 5 10 15 20 25
MAY
JUN
JUL
AUG
SEP

4a

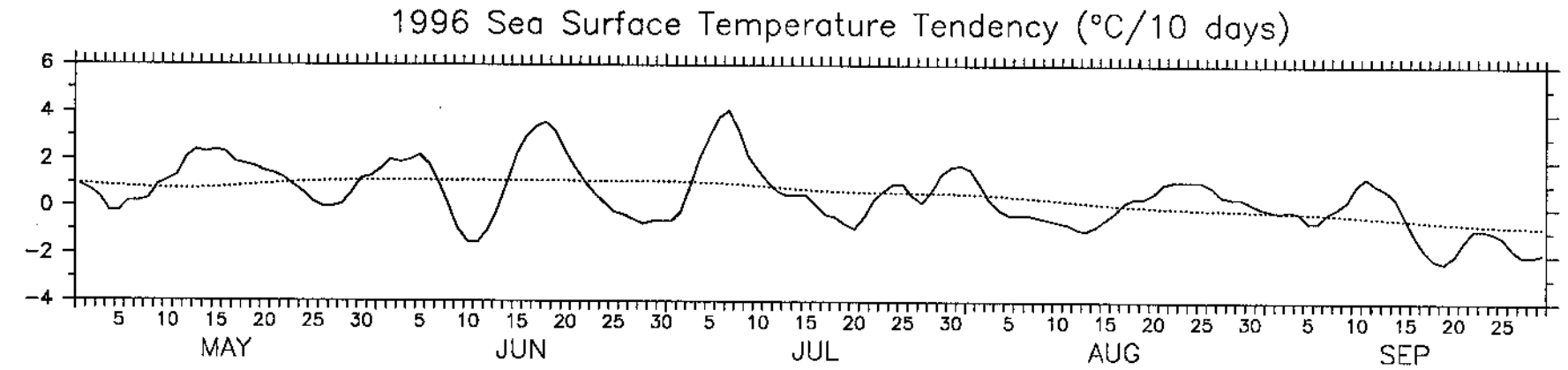
1996 Sea Surface Temperature Tendency (°C/10 days)
6
4
2
0
−2
−4
5 10 15 20 25 30 5 10 15 20 25 30 5 10 15 20 25 30 5 10 15 20 25 30 5 10 15 20 25
MAY
JUN
JUL
AUG
SEP

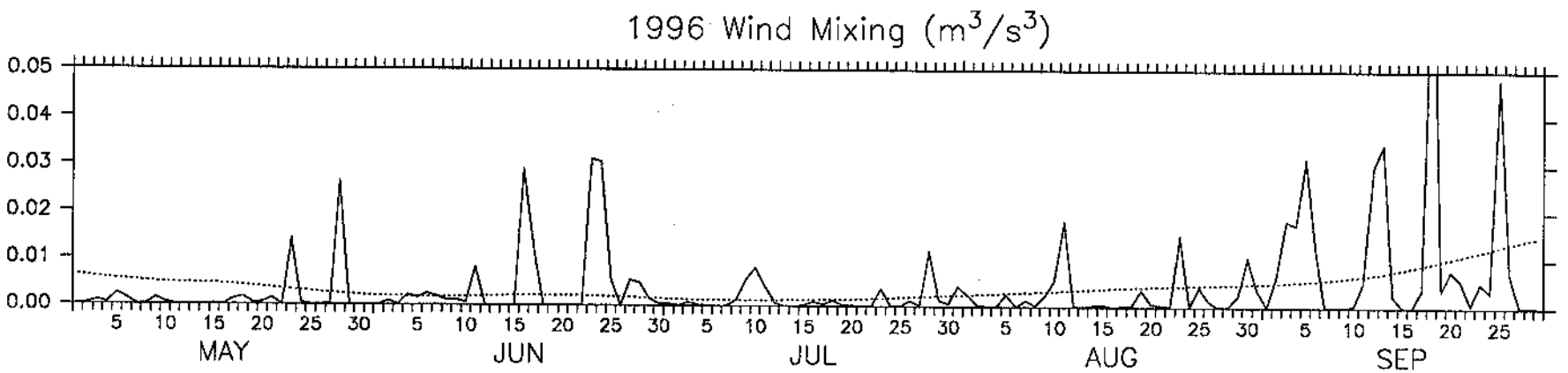
1996 Wind Mixing (m^3/s^3)
0.05
0.04
0.03
0.02
0.01
0.00
5 10 15 20 25 30 5 10 15 20 25 30 5 10 15 20 25 30 5 10 15 20 25 30 5 10 15 20 25
MAY
JUN
JUL
AUG
SEP

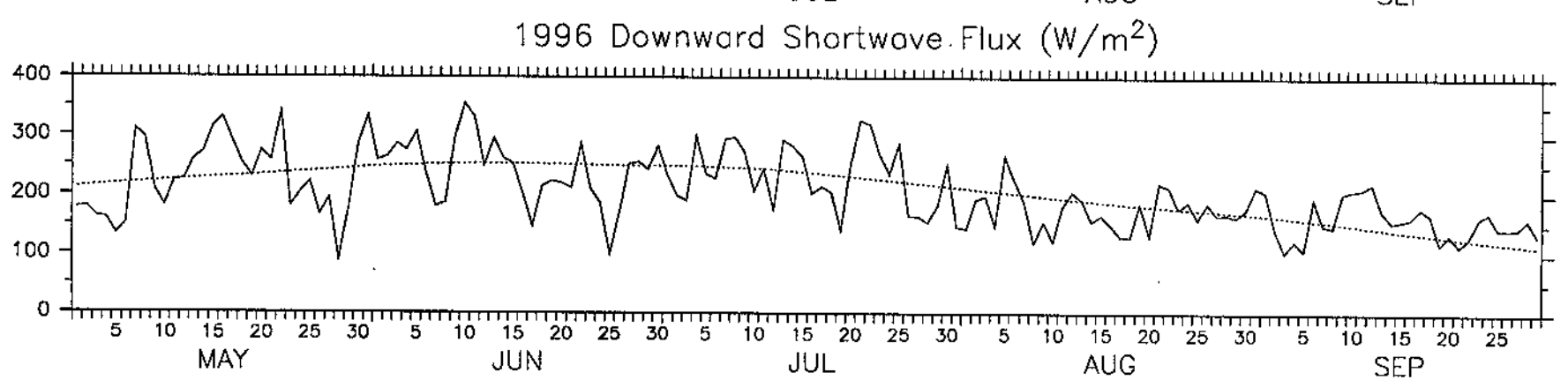
1996 Downward Shortwave Flux (W/m^2)
400
300
200
100
0
5 10 15 20 25 30 5 10 15 20 25 30 5 10 15 20 25 30 5 10 15 20 25 30 5 10 15 20 25
MAY
JUN
JUL
AUG
SEP

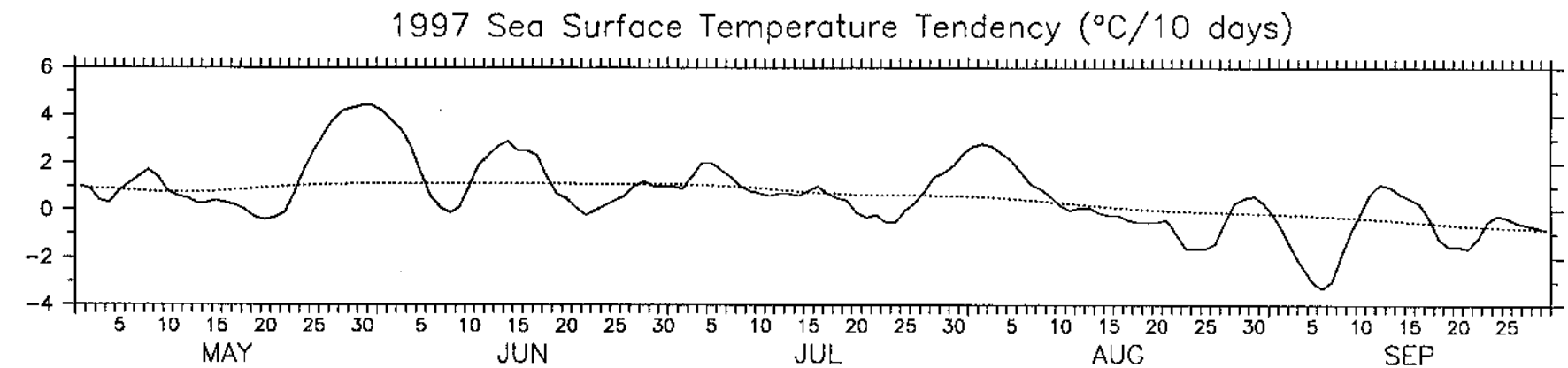
1997 Sea Surface Temperature Tendency (°C/10 days)
6
4
2
0
−2
−4
5 10 15 20 25 30 5 10 15 20 25 30 5 10 15 20 25 30 5 10 15 20 25 30 5 10 15 20 25
MAY
JUN
JUL
AUG
SEP

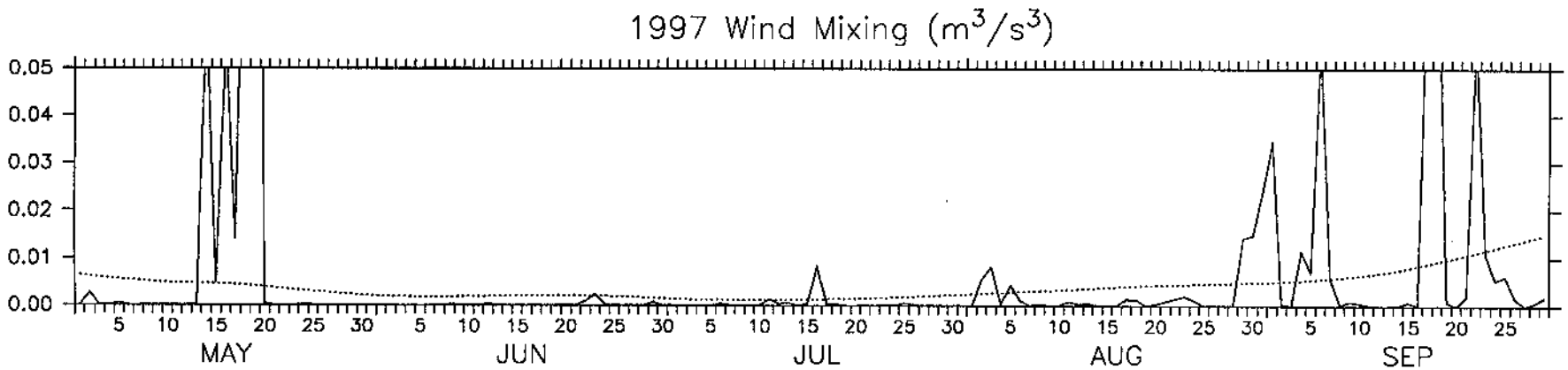
1997 Wind Mixing (m^3/s^3)
0.05
0.04
0.03
0.02
0.01
0.00
5 10 15 20 25 30 5 10 15 20 25 30 5 10 15 20 25 30 5 10 15 20 25 30 5 10 15 20 25
MAY
JUN
JUL
AUG
SEP

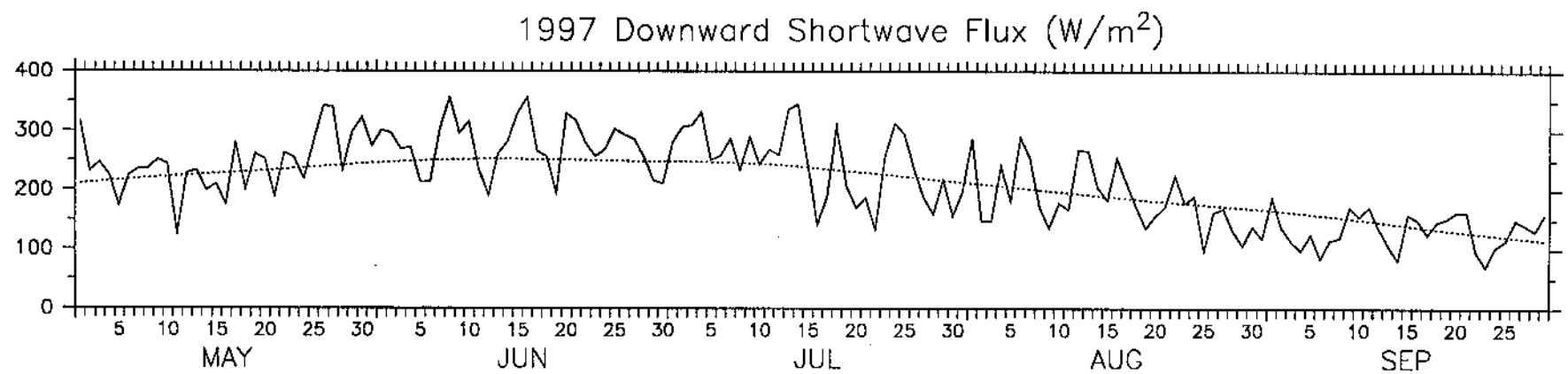
1997 Downward Shortwave Flux (W/m^2)
400
300
200
100
0
5 10 15 20 25 30 5 10 15 20 25 30 5 10 15 20 25 30 5 10 15 20 25 30 5 10 15 20 25
MAY
JUN
JUL
AUG
SEP

4c

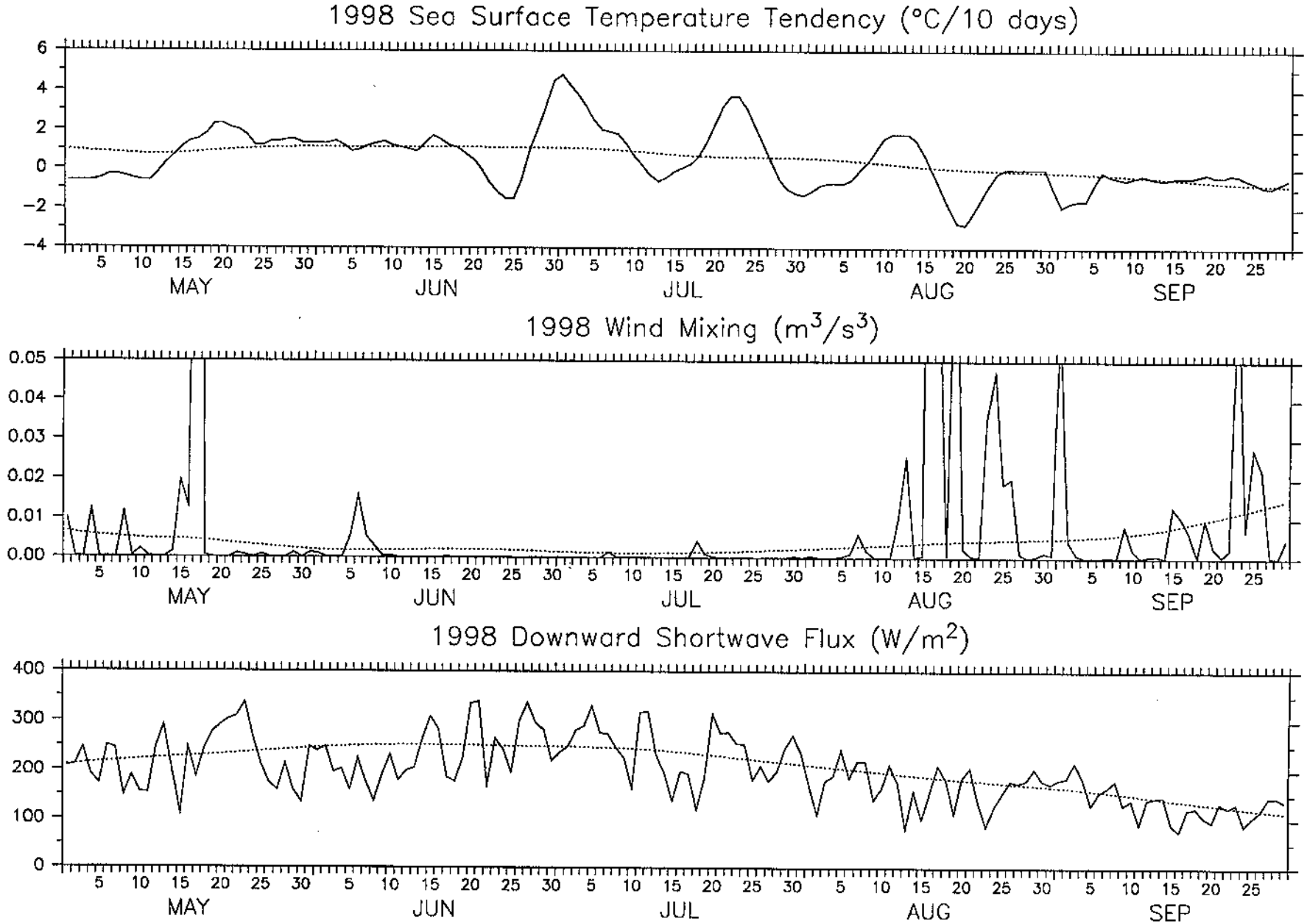
1998 Sea Surface Temperature Tendency (°C/10 days)
6
4
2
0
−2
−4
5 10 15 20 25 30 5 10 15 20 25 30 5 10 15 20 25 30 5 10 15 20 25 30 5 10 15 20 25
MAY
JUN
JUL
AUG
SEP
1998 Wind Mixing (m^3/s^3)
0.05
0.04
0.03
0.02
0.01
0.00
5 10 15 20 25 30 5 10 15 20 25 30 5 10 15 20 25 30 5 10 15 20 25 30 5 10 15 20 25
MAY
JUN
JUL
AUG
SEP
1998 Downward Shortwave Flux (W/m^2)
400
300
200
100
0
5 10 15 20 25 30 5 10 15 20 25 30 5 10 15 20 25 30 5 10 15 20 25 30 5 10 15 20 25
MAY
JUN
JUL
AUG
SEP

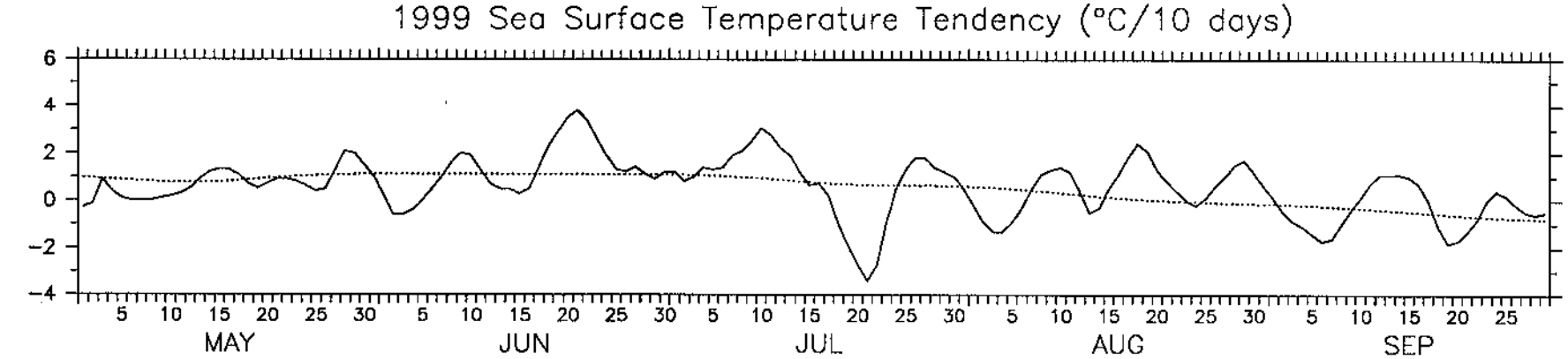
1999 Sea Surface Temperature Tendency (°C/10 days)
6
4
2
0
−2
−4
5 10 15 20 25 30 5 10 15 20 25 30 5 10 15 20 25 30 5 10 15 20 25 30 5 10 15 20 25
MAY
JUN
JUL
AUG
SEP

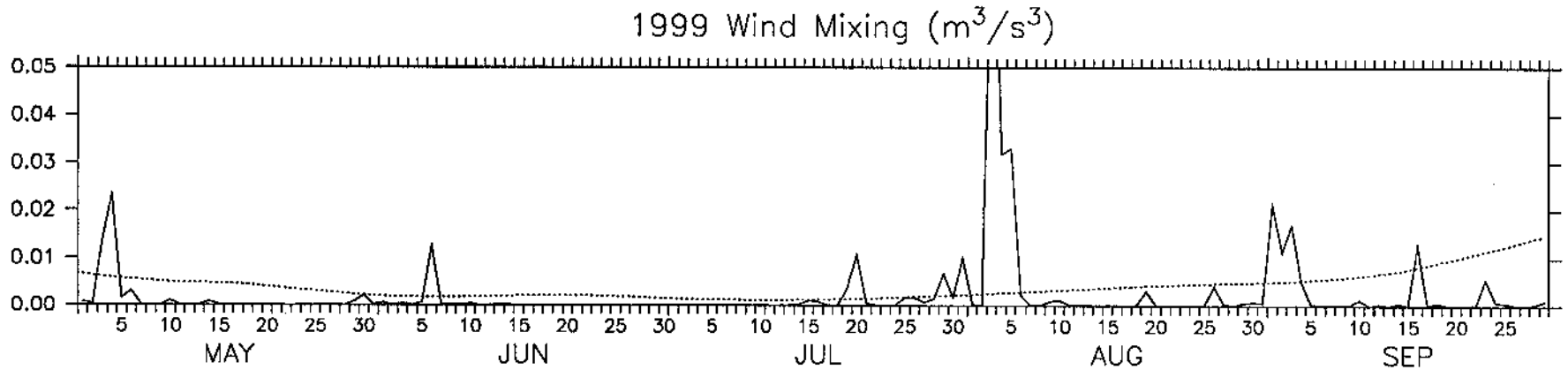
1999 Wind Mixing (m^3/s^3)
0.05
0.04
0.03
0.02
0.01
0.00
5 10 15 20 25 30 5 10 15 20 25 30 5 10 15 20 25 30 5 10 15 20 25 30 5 10 15 20 25
MAY
JUN
JUL
AUG
SEP

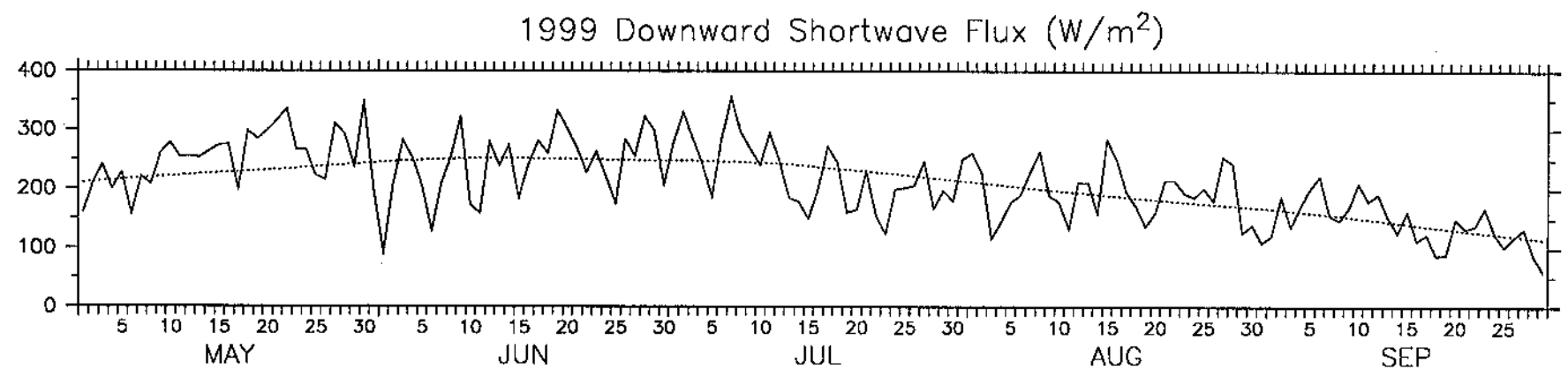
1999 Downward Shortwave Flux (W/m^2)
400
300
200
100
0
5 10 15 20 25 30 5 10 15 20 25 30 5 10 15 20 25 30 5 10 15 20 25 30 5 10 15 20 25
MAY
JUN
JUL
AUG
SEP

4c

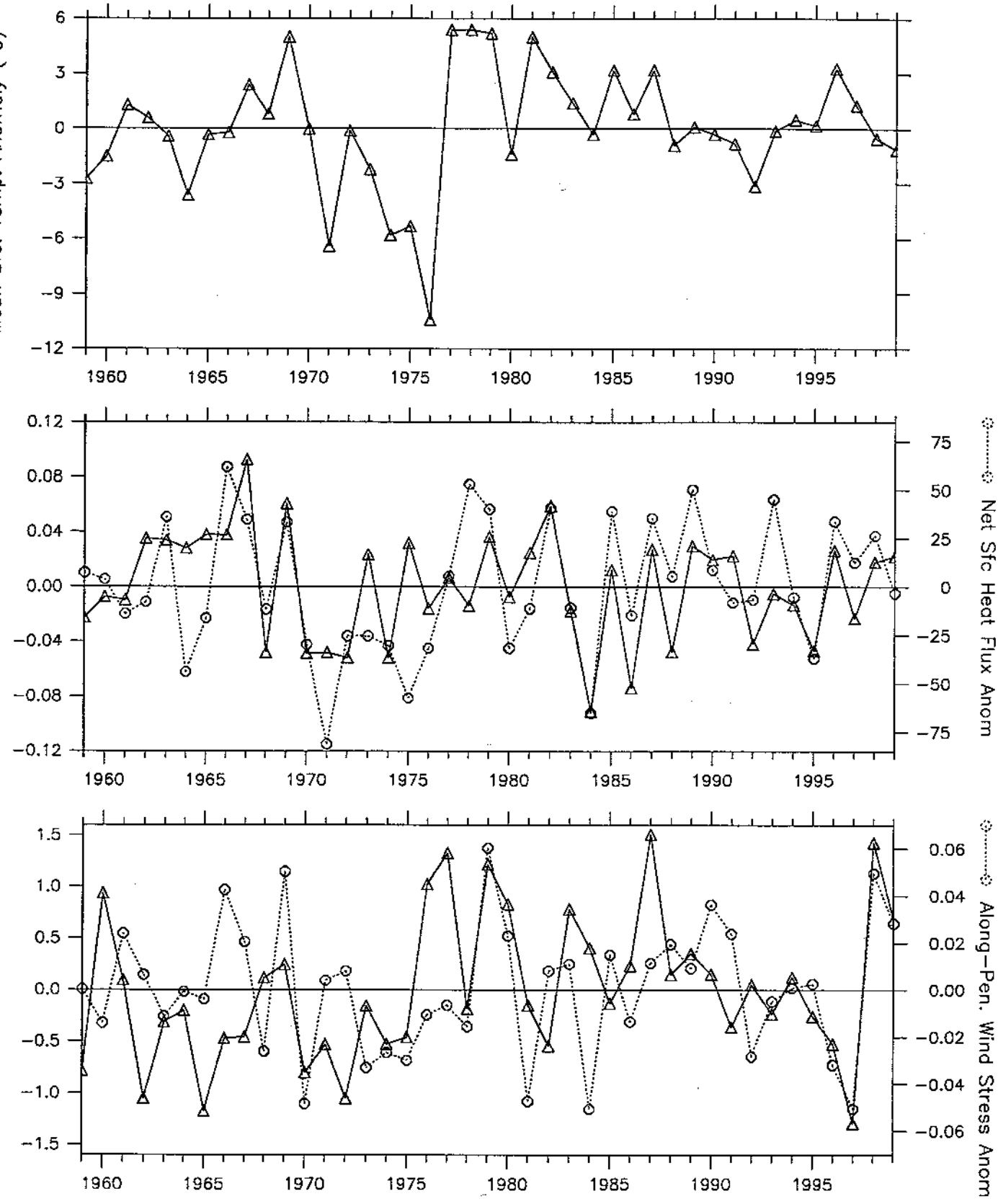
6
3
0
−3
−6
−9
−12
1960
1965
1970
1975
1980
1985
1990
1995
0.12
0.08
0.04
0.00
−0.04
−0.08
−0.12
75
50
25
0
−25
−50
−75
Net Sfc Heat Flux Anom
1.5
1.0
0.5
0.0
−0.5
−1.0
−1.5
0.06
0.04
0.02
0.00
−0.02
−0.04
−0.06
Along−Pen. Wind Stress Anom

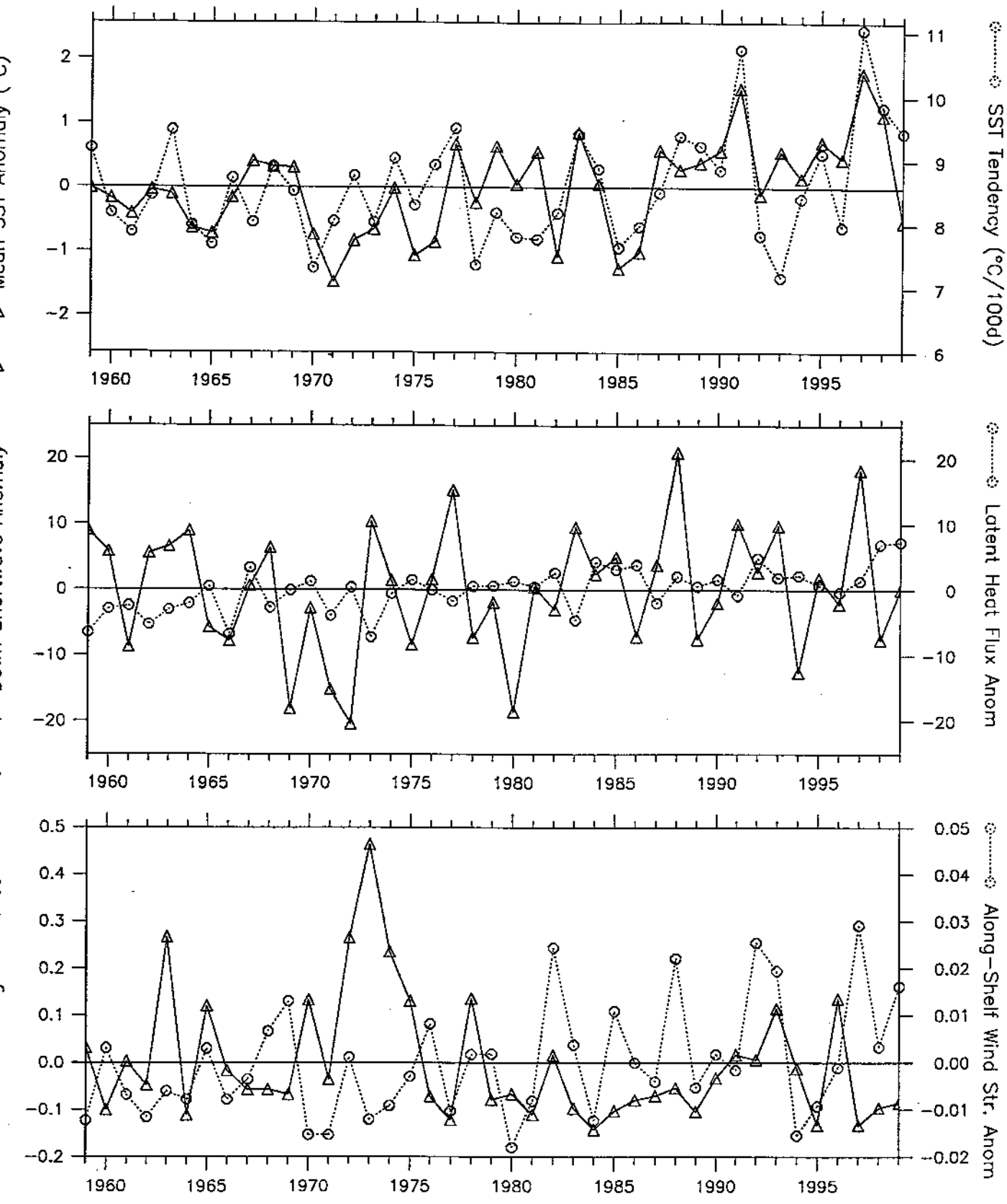
SST Tendency (°C/100d)
Latent Heat Flux Anom
Along-Shelf Wind Str. Anom
1960
1965
1970
1975
1980
1985
1990
1995